

Effective theory approach to new physics in $b \rightarrow u$ and $b \rightarrow c$ leptonic and semileptonic decays.

Rupak Dutta,^{*} Anupama Bhol,[†] and Anjan K. Giri[‡]

*Indian Institute of Technology Hyderabad,
Hyderabad 502205, India*

Abstract

Recent measurements of exclusive $B^- \rightarrow \tau^- \nu$ and $B^0 \rightarrow \pi^+ l^- \bar{\nu}_l$ decays via the $b \rightarrow u l \nu$ transition process differ from the standard model expectation and, if they persist in future B experiments, will be a definite hint of the physics beyond the standard model. Similar hints of new physics have been observed in $b \rightarrow c$ semileptonic transition processes as well. BABAR measures the ratio of branching fractions of $B \rightarrow (D, D^*) \tau \nu$ to the corresponding $B \rightarrow (D, D^*) l \nu$, where l represents either an electron or a muon, and finds 3.4σ discrepancy with the standard model expectation. In this context, we consider a most general effective Lagrangian for the $b \rightarrow u l \nu$ and $b \rightarrow c l \nu$ transition processes in the presence of new physics and perform a combined analysis of all the $b \rightarrow u$ and $b \rightarrow c$ semi-(leptonic) data to explore various new physics operators and their couplings. We consider various new physics scenarios and give predictions for the $B_c \rightarrow \tau \nu$ and $B \rightarrow \pi \tau \nu$ decay branching fractions. We also study the effect of these new physics parameters on the ratio of the branching ratios of $B \rightarrow \pi \tau \nu$ to the corresponding $B \rightarrow \pi l \nu$ decays.

PACS numbers: 14.40.Nd, 13.20.He, 13.20.-v

^{*}Electronic address: rupak@iith.ac.in

[†]Electronic address: ph10p004@iith.ac.in

[‡]Electronic address: giria@iith.ac.in

I. INTRODUCTION

Although, the standard model (SM) of particle physics can explain almost all the existing data to a very good precision, there are some unknowns which are beyond the scope of the SM. The latest discovery of a Higgs-like particle by CMS [1] and ATLAS [2] further confirms the validity of the SM as a low energy effective theory. There are two ways to look for evidence of new physics (NP): direct detection and indirect detection. The Large Hadron Collider (LHC), which is running successfully at CERN, in principle, has the ability to detect new particles that are not within the SM, while, on the other hand the LHCb experiment has the ability to perform indirect searches of NP effects, and since any NP will affect the SM observables, any discrepancy between measurements and the SM expectation will be an indirect evidence of NP beyond the SM.

Recent measurements of $b \rightarrow u \tau \nu$ and $b \rightarrow c \tau \nu$ leptonic and semileptonic B decays differ from SM expectation. The measured branching ratio of $(11.4 \pm 2.2) \times 10^{-5}$ [3–5] for the leptonic $B^- \rightarrow \tau^- \nu$ decay mode is larger than the SM expectation [6–8]. However, the measured branching ratio of $(14.6 \pm 0.7) \times 10^{-5}$ [9–11] for the exclusive semileptonic $B^0 \rightarrow \pi^+ l^- \nu$ decays is consistent with the SM prediction. The SM calculation, however, depends on the hadronic quantities such as B meson decay constant and $B \rightarrow \pi$ transition form factors and the Cabibbo-Kobayashi-Maskawa (CKM) element $|V_{ub}|$. The ratio of branching fractions defined by

$$R_\pi^l = \frac{\tau_{B^0}}{\tau_{B^-}} \frac{\mathcal{B}(B^- \rightarrow \tau^- \nu)}{\mathcal{B}(B^0 \rightarrow \pi^+ l^- \nu)} \quad (1)$$

is independent of the CKM matrix elements and is measured to be (0.73 ± 0.15) [12], and there is still more than 2σ discrepancy with the SM expectation. More recently, BABAR [13] measured the ratio of branching fractions of $B \rightarrow (D, D^*) \tau \nu$ to the corresponding $B \rightarrow (D, D^*) l \nu$ and found 3.4σ discrepancy with the SM expectation [14]. The measured ratios are

$$\begin{aligned} R_D &= \frac{\mathcal{B}(\bar{B} \rightarrow D \tau^- \bar{\nu}_\tau)}{\mathcal{B}(\bar{B} \rightarrow D l^- \bar{\nu}_l)} = 0.440 \pm 0.058 \pm 0.042, \\ R_{D^*} &= \frac{\mathcal{B}(\bar{B} \rightarrow D^* \tau^- \bar{\nu}_\tau)}{\mathcal{B}(\bar{B} \rightarrow D^* l^- \bar{\nu}_l)} = 0.332 \pm 0.024 \pm 0.018, \end{aligned} \quad (2)$$

where the first error is statistical and the second one is systematic. For definiteness, we consider $B^- \rightarrow l^- \bar{\nu}_l$, $\bar{B}^0 \rightarrow \pi^+ l^- \bar{\nu}_l$, $B^- \rightarrow D^0 l^- \bar{\nu}_l$, and $B^- \rightarrow D^{*0} l^- \bar{\nu}_l$ throughout this paper. However, for brevity, we denote all these decay modes as $B \rightarrow l \nu$, $B \rightarrow \pi l \nu$, $B \rightarrow D l \nu$, and $B \rightarrow D^* l \nu$, respectively.

Due to the large mass of the tau lepton, decay processes with a tau lepton in the final state are more sensitive to some new physics effects than processes with first two generation leptons. These NP, in principle, can enhance the decay rate for these helicity-suppressed decay modes quite significantly from the SM prediction. In Ref. [14], a thorough investigation of the lowest dimensional effective operators that leads to modifications in the $B \rightarrow D^* \tau \nu$ decay amplitudes has been done. Possible NP effects on various observables have been explored. Among all the leptonic and semileptonic decays, decays with a tau lepton in the final state can be an excellent probe of new physics as these are sensitive to non-SM contributions arising from the violation of lepton flavor universality (LFU). A model-independent analysis to identify the new physics models has been explored in Ref. [12]. They also look at the possibility of a scalar leptoquark or a vector leptoquark, which can contribute to these decay processes at the tree level and obtain a bound of $m \geq 280 \text{ GeV}$ on the mass of the scalar electroweak triplet leptoquark. Model with composite quarks and leptons also modify these $b \rightarrow u$ and $b \rightarrow c$ semileptonic measurements [12]. The enhanced production of a tau lepton in leptonic and semileptonic decays can be explained by NP contribution with different models among which the minimal supersymmetric standard model (MSSM) is well motivated and is a charming candidate of NP whose Higgs sector contains the two Higgs doublet model (2HDMs). There are four types of 2HDMs such as type-I, type-II, lepton specific, and flipped [15]. New particles such as charged Higgs bosons whose coupling is proportional to the masses of particles in the interaction can have significant effect on decay processes having a tau lepton in the final state. In Ref. [16], the author uses the 2HDM model of type-II for purely leptonic B decays that are sensitive to charged Higgs boson at the tree level. This model, however, cannot explain all the $b \rightarrow c$ semileptonic measurements simultaneously [13]. A lot of studies have been done using the 2HDM of type II and type III models [17]. However, none of the above 2HDMs can accommodate all the existing data on $b \rightarrow u$ and $b \rightarrow c$ semi-(leptonic) decays. Recently, a detailed study of a 2HDM of type III with MSSM-like Higgs potential and flavor-violation in the up sector in Ref. [18] has demonstrated that this model can explain the deviation from the SM in R_π^l , R_D , and R_{D^*} simultaneously and predict enhancement in the $B \rightarrow \tau \nu$, $B \rightarrow D \tau \nu$, and the $B \rightarrow D^* \tau \nu$ decay branching ratios. Also, in Refs. [19, 20], the authors have used a model independent way to analyse the $B \rightarrow D \tau \nu$ and $B \rightarrow D^* \tau \nu$ data by considering an effective theory for the $b \rightarrow c \tau \nu$ processes in the presence of NP and obtain bounds on each NP parameter. They consider two different NP scenarios and see the effect of various NP couplings on different observables. This analysis, however,

does not include the $B \rightarrow \tau\nu$ data. A similar analysis has been performed in Ref. [21] considering a tensor operator in the effective weak Hamiltonian. Also, in Ref. [22], the author investigates the effects of an effective right handed charged currents on the determination of V_{ub} and V_{cb} from inclusive and exclusive B decays. Moreover, the aligned two Higgs doublet model (A2HDM) [23] and, more recently a non-universal left-right model [24] have been explored in order to explain the discrepancies between the measurements and the SM prediction.

The recent measurements suggest the possibility of having new physics in the third generation leptons only. However, more experimental studies are needed to confirm the presence of NP. A thorough investigation of these decays will enable us to have significant constraints on NP scenarios. In this report, we use the most general effective Lagrangian for the $b \rightarrow q$ semi-(leptonic) transition decays and do a combined analysis of $b \rightarrow u$ and $b \rightarrow c$ semi-(leptonic) decay processes where we use constraints from all the existing data related to these decays. It differs considerably from earlier treatments. First, we have introduced the right-handed neutrinos and their interactions for our analysis. Second, we have performed a combined analysis of all the $b \rightarrow u$ and $b \rightarrow c$ data. We illustrate four different scenarios of the new physics and the effects of each NP coupling on various observables are shown. We predict the branching ratio of $B_c \rightarrow \tau\nu$ and $B \rightarrow \pi\tau\nu$ decay processes in all four different scenarios. We also consider the ratio of branching ratio R_π of $B \rightarrow \pi\tau\nu$ to the corresponding $B \rightarrow \pi l\nu$ decay mode for our analysis.

The paper is organized as follows. In Sec. II, we start with a brief description of the effective Lagrangian for the $b \rightarrow (u, c)l\nu$ processes and then present all the relevant formulae of the decay rates for various decay modes in the presence of various NP couplings. We then define several observables in $B \rightarrow \pi\tau\nu$, $B \rightarrow D\tau\nu$, and $B \rightarrow D^*\tau\nu$ decays. The numerical prediction for various NP couplings and the effects of each NP coupling on various observables are presented in Sec. III. We also discuss the effects of these NP couplings on $\mathcal{B}(B_c \rightarrow \tau\nu)$, $\mathcal{B}(B \rightarrow \pi\tau\nu)$, and the ratio R_π for various NP scenarios in this section. We conclude with a summary of our results in Sec. IV. We report the details of the kinematics and various form factors in the Appendix.

II. EFFECTIVE LAGRANGIAN AND DECAY AMPLITUDE

The most general effective Lagrangian for $b \rightarrow q' l \nu$ in presence of NP, where $q' = u, c$, can be written as [25, 26]

$$\begin{aligned} \mathcal{L}_{\text{eff}} = & -\frac{g^2}{2M_W^2} V_{q'b} \left\{ (1 + V_L) \bar{l}_L \gamma_\mu \nu_L \bar{q}'_L \gamma^\mu b_L + V_R \bar{l}_L \gamma_\mu \nu_L \bar{q}'_R \gamma^\mu b_R \right. \\ & + \tilde{V}_L \bar{l}_R \gamma_\mu \nu_R \bar{q}'_L \gamma^\mu b_L + \tilde{V}_R \bar{l}_R \gamma_\mu \nu_R \bar{q}'_R \gamma^\mu b_R \\ & + S_L \bar{l}_R \nu_L \bar{q}'_R b_L + S_R \bar{l}_R \nu_L \bar{q}'_L b_R \\ & + \tilde{S}_L \bar{l}_L \nu_R \bar{q}'_R b_L + \tilde{S}_R \bar{l}_L \nu_R \bar{q}'_L b_R \\ & \left. + T_L \bar{l}_R \sigma_{\mu\nu} \nu_L \bar{q}'_R \sigma^{\mu\nu} b_L + \tilde{T}_L \bar{l}_L \sigma_{\mu\nu} \nu_R \bar{q}'_L \sigma^{\mu\nu} b_R \right\} + \text{h.c.}, \end{aligned} \quad (3)$$

where g is the weak coupling constant which can be related to the Fermi constant by the relation $g^2/8M_W^2 = G_F/\sqrt{2}$ and $V_{q'b}$ is the CKM Matrix elements. The new physics couplings denoted by $V_{L,R}$, $S_{L,R}$, and T_L involve left-handed neutrinos, whereas, the NP couplings denoted by $\tilde{V}_{L,R}$, $\tilde{S}_{L,R}$, and \tilde{T}_L involve right-handed neutrinos. We assume the NP couplings to be real for our analysis. Again, the projection operators are $P_L = (1 - \gamma_5)/2$ and $P_R = (1 + \gamma_5)/2$. We neglect the new physics effects coming from the tensor couplings T_L and \tilde{T}_L for our analysis. With this simplification, we obtain

$$\begin{aligned} \mathcal{L}_{\text{eff}} = & -\frac{G_F}{\sqrt{2}} V_{q'b} \left\{ G_V \bar{l} \gamma_\mu (1 - \gamma_5) \nu_l \bar{q}' \gamma^\mu b - G_A \bar{l} \gamma_\mu (1 - \gamma_5) \nu_l \bar{q}' \gamma^\mu \gamma_5 b \right. \\ & + G_S \bar{l} (1 - \gamma_5) \nu_l \bar{q}' b - G_P \bar{l} (1 - \gamma_5) \nu_l \bar{q}' \gamma_5 b \\ & + \tilde{G}_V \bar{l} \gamma_\mu (1 + \gamma_5) \nu_l \bar{q}' \gamma^\mu b - \tilde{G}_A \bar{l} \gamma_\mu (1 + \gamma_5) \nu_l \bar{q}' \gamma^\mu \gamma_5 b \\ & \left. + \tilde{G}_S \bar{l} (1 + \gamma_5) \nu_l \bar{q}' b - \tilde{G}_P \bar{l} (1 + \gamma_5) \nu_l \bar{q}' \gamma_5 b \right\} + \text{h.c.}, \end{aligned} \quad (4)$$

where

$$\begin{aligned} G_V &= 1 + V_L + V_R, & G_A &= 1 + V_L - V_R, \\ G_S &= S_L + S_R, & G_P &= S_L - S_R, \\ \tilde{G}_V &= \tilde{V}_L + \tilde{V}_R, & \tilde{G}_A &= \tilde{V}_L - \tilde{V}_R, \\ \tilde{G}_S &= \tilde{S}_L + \tilde{S}_R, & \tilde{G}_P &= \tilde{S}_L - \tilde{S}_R. \end{aligned} \quad (5)$$

In the SM, $G_V = G_A = 1$ and all other NP couplings are zero.

The expressions for $B \rightarrow l\nu$, $B \rightarrow Pl\nu$, and $B \rightarrow Vl\nu$ decay amplitude depends on nonperturbative hadronic matrix elements that can be expressed in terms of B_q meson decay constants and $B \rightarrow (P, V)$ transition form factors, where P denotes a pseudoscalar meson and V denotes a vector meson, respectively. The B meson decay constant and $B \rightarrow (P, V)$ transition form factors are defined as

$$\begin{aligned}
\langle 0 | \bar{q}' \gamma_\mu \gamma_5 b | B(p) \rangle &= -i f_{B_{q'}} p_\mu, \\
\langle P(p') | \bar{q}' \gamma_\mu b | B(p) \rangle &= F_+(q^2) \left[(p + p')_\mu - \frac{m_B^2 - m_P^2}{q^2} q_\mu \right] + F_0(q^2) \frac{m_B^2 - m_P^2}{q^2} q_\mu, \\
\langle V(p', \epsilon^*) | \bar{q}' \gamma_\mu b | B(p) \rangle &= \frac{2i V(q^2)}{m_B + m_V} \varepsilon_{\mu\nu\rho\sigma} \epsilon^{*\nu} p'^\rho p^\sigma, \\
\langle V(p', \epsilon^*) | \bar{q}' \gamma_\mu \gamma_5 b | B(p) \rangle &= 2m_V A_0(q^2) \frac{\epsilon^* \cdot q}{q^2} q_\mu + (m_B + m_V) A_1(q^2) \left[\epsilon_\mu^* - \frac{\epsilon^* \cdot q}{q^2} q_\mu \right] \\
&\quad - A_2(q^2) \frac{\epsilon^* \cdot q}{(m_B + m_V)} \left[(p + p')_\mu - \frac{m_B^2 - m_V^2}{q^2} q_\mu \right], \tag{6}
\end{aligned}$$

where $q = p - p'$ is the momentum transfer. Again, from Lorentz invariance and parity, we obtain

$$\begin{aligned}
\langle 0 | \bar{q}' \gamma_\mu b | B(p) \rangle &= 0, \\
\langle P(p') | \bar{q}' \gamma_\mu \gamma_5 b | B(p) \rangle &= 0, \\
\langle V(p', \epsilon^*) | \bar{q}' b | B(p) \rangle &= 0. \tag{7}
\end{aligned}$$

We use the equation of motion to find the scalar and pseudoscalar matrix elements. That is

$$\begin{aligned}
\langle 0 | \bar{q}' \gamma_5 b | B(p) \rangle &= i \frac{m_B^2}{m_b(\mu) + m_{q'}(\mu)} f_{B_{q'}}, \\
\langle P(p') | \bar{q}' b | B(p) \rangle &= \frac{m_B^2 - m_P^2}{m_b(\mu) - m_{q'}(\mu)} F_0(q^2), \\
\langle V(p', \epsilon^*) | \bar{q}' \gamma_5 b | B(p) \rangle &= - \frac{2m_V A_0(q^2)}{m_b(\mu) + m_{q'}(\mu)} \epsilon^* \cdot q, \tag{8}
\end{aligned}$$

where, for the $B \rightarrow \pi$ form factors, we use the formulae and the input values reported in Ref. [27]. Similarly, we follow Refs. [28–30] and employ heavy quark effective theory (HQET) to estimate the $B \rightarrow D$ and $B \rightarrow D^*$ form factors. All the relevant formulae and various input parameters pertinent to our analysis are presented in Appendix. B and in Appendix. C.

Using the effective Lagrangian of Eq. (4) in the presence of NP, the partial decay width of $B \rightarrow l\nu$ can be expressed as

$$\Gamma(B \rightarrow l\nu) = \frac{G_F^2 |V_{ub}|^2}{8\pi} f_B^2 m_l^2 m_B \left(1 - \frac{m_l^2}{m_B^2}\right)^2 \left\{ \left[G_A - \frac{m_B^2}{m_l(m_b(\mu) + m_u(\mu))} G_P \right]^2 \right.$$

$$+ \left[\tilde{G}_A - \frac{m_B^2}{m_l (m_b(\mu) + m_u(\mu))} \tilde{G}_P \right]^2 \Big\}, \quad (9)$$

where, in the SM, we have $G_A = 1$ and $G_P = \tilde{G}_A = \tilde{G}_P = 0$, so that

$$\Gamma(B \rightarrow l \nu)_{\text{SM}} = \frac{G_F^2 |V_{ub}|^2}{8 \pi} f_B^2 m_l^2 m_B \left(1 - \frac{m_l^2}{m_B^2}\right)^2. \quad (10)$$

It is important to note that the right-handed neutrino couplings denoted by $\tilde{V}_{L,R}$ and $\tilde{S}_{L,R}$ appear in the decay width quadratically, whereas, the left-handed neutrino couplings denoted by $V_{L,R}$ and $S_{L,R}$ appear linearly in the decay rates. The linear dependence, arising due to the interference between the SM couplings and the NP couplings, is suppressed for the right-handed neutrino couplings as it is proportional to a small factor m_ν and hence is neglected. We now proceed to discuss the $B \rightarrow P l \nu$ and $B \rightarrow V l \nu$ decays.

We follow the helicity methods of Refs. [31, 32] for the $B \rightarrow P l \nu$ and $B \rightarrow V l \nu$ semileptonic decays. The differential decay distribution can be written as

$$\frac{d\Gamma}{dq^2 d\cos\theta_l} = \frac{G_F^2 |V_{q'b}|^2 |\vec{p}_{(P,V)}|}{2^9 \pi^3 m_B^2} \left(1 - \frac{m_l^2}{q^2}\right) L_{\mu\nu} H^{\mu\nu}, \quad (11)$$

where $L_{\mu\nu}$ and $H_{\mu\nu}$ are the usual leptonic and hadronic tensors, respectively. Here, θ_l is the angle between the P (V) meson and the lepton three momentum vector in the q^2 rest frame. The three momentum vector $|\vec{p}_{(P,V)}|$ is defined as $|\vec{p}_{(P,V)}| = \sqrt{\lambda(m_B^2, m_{P(V)}^2, q^2)}/2m_B$, where $\lambda(a, b, c) = a^2 + b^2 + c^2 - 2(ab + bc + ca)$. The resulting differential decay distribution for $B \rightarrow P l \nu$ in terms of the helicity amplitudes H_0 , H_t , and H_S is

$$\begin{aligned} \frac{d\Gamma}{dq^2 d\cos\theta_l} = 2 N |\vec{p}_P| & \left\{ H_0^2 \sin^2 \theta_l (G_V^2 + \tilde{G}_V^2) + \frac{m_l^2}{q^2} \left[H_0 G_V \cos \theta_l - \left(H_t G_V + \frac{\sqrt{q^2}}{m_l} H_S G_S \right) \right]^2 \right. \\ & \left. + \frac{m_l^2}{q^2} \left[H_0 \tilde{G}_V \cos \theta_l - \left(H_t \tilde{G}_V + \frac{\sqrt{q^2}}{m_l} H_S \tilde{G}_S \right) \right]^2 \right\}, \end{aligned} \quad (12)$$

where

$$\begin{aligned} N &= \frac{G_F^2 |V_{q'b}|^2 q^2}{256 \pi^3 m_B^2} \left(1 - \frac{m_l^2}{q^2}\right)^2, \\ H_0 &= \frac{2 m_B |\vec{p}_P|}{\sqrt{q^2}} F_+(q^2), \\ H_t &= \frac{m_B^2 - m_P^2}{\sqrt{q^2}} F_0(q^2), \\ H_S &= \frac{m_B^2 - m_P^2}{m_b(\mu) - m_{q'}(\mu)} F_0(q^2). \end{aligned} \quad (13)$$

The details of the helicity amplitudes calculation are given in Appendix. A. We refer to Refs. [31, 32] for all omitted details. We determine the differential decay rate $d\Gamma/dq^2$ by performing the $\cos\theta_l$ integration, i.e,

$$\begin{aligned} \frac{d\Gamma^P}{dq^2} = & \frac{8N|\vec{p}_P|}{3} \left\{ H_0^2 (G_V^2 + \tilde{G}_V^2) \left(1 + \frac{m_l^2}{2q^2}\right) \right. \\ & \left. + \frac{3m_l^2}{2q^2} \left[\left(H_t G_V + \frac{\sqrt{q^2}}{m_l} H_S G_S\right)^2 + \left(H_t \tilde{G}_V + \frac{\sqrt{q^2}}{m_l} H_S \tilde{G}_S\right)^2 \right] \right\}, \end{aligned} \quad (14)$$

where, in the SM, $G_V = 1$ and all other couplings are zero. One obtains

$$\left(\frac{d\Gamma^P}{dq^2}\right)_{\text{SM}} = \frac{8N|\vec{p}_P|}{3} \left\{ H_0^2 \left(1 + \frac{m_l^2}{2q^2}\right) + \frac{3m_l^2}{2q^2} H_t^2 \right\}. \quad (15)$$

Our formulae for the differential branching ratio in the presence of NP couplings in Eq. (12) and Eq. (14) differ slightly from those given in Ref. [19]. The term containing G_S and \tilde{G}_S is positive in Eq. (12) and Eq. (14), whereas, it is negative in Ref. [19]. Although, the SM formula is same, the numerical differences may not be negligible once the NP couplings $S_{L,R}$ and $\tilde{S}_{L,R}$ are introduced. It is worth mentioning that, for $l = e, \mu$, the term containing m_l^2/q^2 can be safely ignored. However, same is not true for the $B \rightarrow P\tau\nu$ decay mode as the mass of τ lepton is quite large and one cannot neglect the m_τ^2/q^2 term from the decay amplitude. We assume that the NP affects the third generation lepton only.

Similarly, the differential decay distribution for $B \rightarrow V l \nu$ in terms of the helicity amplitudes $\mathcal{A}_0, \mathcal{A}_\parallel, \mathcal{A}_\perp, \mathcal{A}_P$, and \mathcal{A}_t is

$$\begin{aligned} \frac{d\Gamma}{dq^2 d\cos\theta_l} = & N|\vec{p}_V| \left\{ 2\mathcal{A}_0^2 \sin^2\theta_l (G_A^2 + \tilde{G}_A^2) + (1 + \cos^2\theta_l) [\mathcal{A}_\parallel^2 (G_A^2 + \tilde{G}_A^2) + \mathcal{A}_\perp^2 (G_V^2 + \tilde{G}_V^2)] \right. \\ & - 4\mathcal{A}_\parallel \mathcal{A}_\perp \cos\theta_l (G_A G_V - \tilde{G}_A \tilde{G}_V) + \frac{m_l^2}{q^2} \sin^2\theta_l [\mathcal{A}_\parallel^2 (G_A^2 + \tilde{G}_A^2) + \mathcal{A}_\perp^2 (G_V^2 + \tilde{G}_V^2)] \\ & + \frac{2m_l^2}{q^2} \left[\left\{ \mathcal{A}_0 G_A \cos\theta_l - \left(\mathcal{A}_t G_A + \frac{\sqrt{q^2}}{m_l} \mathcal{A}_P G_P \right) \right\}^2 \right. \\ & \left. \left. + \left\{ \mathcal{A}_0 \tilde{G}_A \cos\theta_l - \left(\mathcal{A}_t \tilde{G}_A + \frac{\sqrt{q^2}}{m_l} \mathcal{A}_P \tilde{G}_P \right) \right\}^2 \right] \right\}, \end{aligned} \quad (16)$$

where

$$\begin{aligned} \mathcal{A}_0 &= \frac{1}{2m_V \sqrt{q^2}} \left[(m_B^2 - m_V^2 - q^2)(m_B + m_V) A_1(q^2) - \frac{4M_B^2 |\vec{p}_V|^2}{m_B + m_V} A_2(q^2) \right], \\ \mathcal{A}_\parallel &= \frac{2(m_B + m_V) A_1(q^2)}{\sqrt{2}}, \end{aligned}$$

$$\begin{aligned}
\mathcal{A}_\perp &= -\frac{4m_B V(q^2) |\vec{p}_V|}{\sqrt{2}(m_B + m_V)}, \\
\mathcal{A}_t &= \frac{2m_B |\vec{p}_V| A_0(q^2)}{\sqrt{q^2}}, \\
\mathcal{A}_P &= -\frac{2m_B |\vec{p}_V| A_0(q^2)}{(m_b(\mu) + m_c(\mu))}.
\end{aligned} \tag{17}$$

We perform the $\cos \theta_l$ integration and obtain the differential decay rate $d\Gamma/dq^2$, that is

$$\frac{d\Gamma^V}{dq^2} = \frac{8N |\vec{p}_V|}{3} \left\{ \mathcal{A}_{AV}^2 + \frac{m_l^2}{2q^2} [\mathcal{A}_{AV}^2 + 3\mathcal{A}_{tP}^2] + \tilde{\mathcal{A}}_{AV}^2 + \frac{m_l^2}{2q^2} [\tilde{\mathcal{A}}_{AV}^2 + 3\tilde{\mathcal{A}}_{tP}^2] \right\}, \tag{18}$$

where

$$\begin{aligned}
\mathcal{A}_{AV}^2 &= \mathcal{A}_0^2 G_A^2 + \mathcal{A}_\parallel^2 G_A^2 + \mathcal{A}_\perp^2 G_V^2, \\
\tilde{\mathcal{A}}_{AV}^2 &= \mathcal{A}_0^2 \tilde{G}_A^2 + \mathcal{A}_\parallel^2 \tilde{G}_A^2 + \mathcal{A}_\perp^2 \tilde{G}_V^2, \\
\mathcal{A}_{tP} &= \mathcal{A}_t G_A + \frac{\sqrt{q^2}}{m_l} \mathcal{A}_P G_P, \\
\tilde{\mathcal{A}}_{tP} &= \mathcal{A}_t \tilde{G}_A + \frac{\sqrt{q^2}}{m_l} \mathcal{A}_P \tilde{G}_P.
\end{aligned} \tag{19}$$

In the SM, $G_V = G_A = 1$ and all other NP couplings are zero. We obtain

$$\left(\frac{d\Gamma^V}{dq^2} \right)_{\text{SM}} = \frac{8N |\vec{p}_V|}{3} \left\{ (\mathcal{A}_0^2 + \mathcal{A}_\parallel^2 + \mathcal{A}_\perp^2) \left(1 + \frac{m_l^2}{2q^2} \right) + \frac{3m_l^2}{2q^2} \mathcal{A}_t^2 \right\}. \tag{20}$$

We want to mention that our formulae for the $B \rightarrow V l \nu$ differential decay width in Eq. (16) and Eq. (18) differ slightly from those reported in Ref. [19]. Our formulae, however, agree with those reported in Ref. [14]. In Eq. (16), we have $(1 + \cos^2 \theta_l)$ instead of $(1 + \cos \theta_l)^2$ reported in Ref. [19]. Again, note that our definition of $G_P = S_L - S_R$, different from that of $g_P = S_R - S_L$ [19], leads to a sign discrepancy in \mathcal{A}_{tP} ($\tilde{\mathcal{A}}_{tP}$). Depending on the NP couplings G_P and \tilde{G}_P , the numerical estimates might differ from Ref. [19].

We define some physical observables such as differential branching ratio $\text{DBR}(q^2)$, the ratio of branching fractions $R(q^2)$, and the forward-backward asymmetry $A_{FB}(q^2)$.

$$\begin{aligned}
\text{DBR}(q^2) &= \left(\frac{d\Gamma}{dq^2} \right) / \Gamma_{\text{tot}}, & R(q^2) &= \frac{\text{DBR}(q^2) (B \rightarrow (P, V) \tau \nu)}{\text{DBR}(q^2) (B \rightarrow (P, V) l \nu)}, \\
[A_{FB}]_{(P, V)}(q^2) &= \frac{\left(\int_{-1}^0 - \int_0^1 \right) d \cos \theta_l \frac{d\Gamma^{(P, V)}}{dq^2 d \cos \theta_l}}{\frac{d\Gamma^{(P, V)}}{dq^2}}.
\end{aligned} \tag{21}$$

For $B \rightarrow Pl\nu$ decay mode, the forward-backward asymmetry in the presence of NP is

$$A_{FB}^P(q^2) = \frac{3m_l^2}{2q^2} \frac{H_0 G_V \left[\left(H_t G_V + \frac{\sqrt{q^2}}{m_l} H_S G_S \right) + \left(H_t \tilde{G}_V + \frac{\sqrt{q^2}}{m_l} H_S \tilde{G}_S \right) \right]}{H_0^2 (G_V^2 + \tilde{G}_V^2) \left(1 + \frac{m_l^2}{2q^2} \right) + \frac{3m_l^2}{2q^2} \left[\left(H_t G_V + \frac{\sqrt{q^2}}{m_l} H_S G_S \right)^2 + \left(H_t \tilde{G}_V + \frac{\sqrt{q^2}}{m_l} H_S \tilde{G}_S \right)^2 \right]}, \quad (22)$$

where, in the SM, $G_V = 1$ and all other couplings are zero. We obtain

$$(A_{FB}^P)_{\text{SM}}(q^2) = \frac{3m_l^2}{2q^2} \frac{H_0 H_t}{H_0^2 \left(1 + \frac{m_l^2}{2q^2} \right) + \frac{3m_l^2}{2q^2} H_t^2}. \quad (23)$$

Similarly, for $B \rightarrow V l \nu$ decay mode, in the presence of NP

$$A_{FB}^V(q^2) = \frac{3}{2} \frac{\mathcal{A}_{\parallel} \mathcal{A}_{\perp} (G_A G_V - \tilde{G}_A \tilde{G}_V) + \frac{m_l^2}{q^2} \mathcal{A}_0 G_A \left[\mathcal{A}_t G_A - \frac{\sqrt{q^2}}{m_l} \mathcal{A}_P G_P + \mathcal{A}_t \tilde{G}_A - \frac{\sqrt{q^2}}{m_l} \mathcal{A}_P \tilde{G}_P \right]}{\mathcal{A}_{AV}^2 + \frac{m_l^2}{2q^2} [\mathcal{A}_{AV}^2 + 3\mathcal{A}_{tP}^2] + \tilde{\mathcal{A}}_{AV}^2 + \frac{m_l^2}{2q^2} [\tilde{\mathcal{A}}_{AV}^2 + 3\tilde{\mathcal{A}}_{tP}^2]}. \quad (24)$$

In the SM, $G_A = G_V = 1$ while all other NP couplings are zero. Thus we obtain

$$(A_{FB}^V)_{\text{SM}}(q^2) = \frac{3}{2} \frac{\mathcal{A}_{\parallel} \mathcal{A}_{\perp} + \frac{m_l^2}{q^2} \mathcal{A}_0 \mathcal{A}_t}{\left\{ (\mathcal{A}_0^2 + \mathcal{A}_{\parallel}^2 + \mathcal{A}_{\perp}^2) \left(1 + \frac{m_l^2}{2q^2} \right) + \frac{3m_l^2}{2q^2} \mathcal{A}_t^2 \right\}}. \quad (25)$$

We see that, in the SM, for the light leptons $l = e, \mu$, the forward-backward asymmetry is vanishingly small due to the m_l^2/q^2 term for the $B \rightarrow Pl\nu$ decay modes. However, for $B \rightarrow V l \nu$, the first term will contribute and we will get a nonzero value for the forward-backward asymmetry. Any non-zero value of the A_{FB} parameter for the $B \rightarrow Pl\nu$ decay modes will be a hint of NP in all generation leptons. We, however, ignore the NP effects in the case of $l = e, \mu$. We strictly assume that only third generation leptons get modified due to NP couplings.

We wish to determine various NP effects in a model independent way. The theoretical uncertainties in the calculation of the decay branching fractions come from various input parameters. first, there are uncertainties associated with well-known input parameters such as quark masses, meson masses, and lifetime of the mesons. We ignore these uncertainties as these are not important for our analysis. Second, there are uncertainties that are associated with not so well-known hadronic input parameters such as form factors, decay constants, and the CKM elements. In order to realize the effect of the above-mentioned uncertainties on various observables, we use a random number generator and perform a random scan of all the allowed hadronic as well as the CKM elements.

In our random scan of the theoretical parameter space, we vary all the hadronic inputs such as $B \rightarrow (P, V)$ form factors, f_{B_q} decay constants, and CKM elements $|V_{qb}|$ within 3σ from their central values. In order to determine the allowed NP parameter space, we impose the experimental constraints coming from the measured ratio of branching fractions R_π^l , R_D , and R_{D^*} simultaneously. This is to ensure that the resulting NP parameter space can simultaneously accommodate all the existing data on $b \rightarrow u$ and $b \rightarrow c$ leptonic and semileptonic decays. We impose the experimental constraints in such a way that we ignore those theoretical models that are not compatible within 3σ of the experimental constraints for the 3σ random scan.

III. RESULTS AND DISCUSSION

For definiteness, we summarize the input parameters for our numerical analysis. We use the following inputs from Ref. [5].

$$\begin{aligned}
m_b &= 4.18 \text{ GeV}, & m_c &= 1.275 \text{ GeV}, & m_\pi &= 0.13957 \text{ GeV}, \\
m_{B^-} &= 5.27925 \text{ GeV}, & m_{B^0} &= 5.27955 \text{ GeV}, & m_{B_c} &= 6.277 \text{ GeV}, \\
m_{D^0} &= 1.86486 \text{ GeV}, & m_{D^{*0}} &= 2.00698 \text{ GeV}, & \tau_{B^0} &= 1.519 \times 10^{-12} \text{ Sec}, \\
\tau_{B^-} &= 1.641 \times 10^{-12} \text{ Sec}, & \tau_{B_c} &= 0.453 \times 10^{-12} \text{ Sec}, & &
\end{aligned} \tag{26}$$

where $m_b \equiv m_b(m_b)$ and $m_c \equiv m_c(m_c)$ denote the running b and c quark masses in $\overline{\text{MS}}$ scheme. We employ a renormalization scale $\mu = m_b$ for which the strong coupling constant $\alpha_s(m_b) = 0.224$. Using the two-loop expression for the running quark mass [33], we find $m_c(m_b) = 0.91 \text{ GeV}$. Thus, the coefficients $V_{L,R}$, $\tilde{V}_{L,R}$, $S_{L,R}$, and $\tilde{S}_{L,R}$ are defined at the scale $\mu = m_b$. The error associated with the quark masses, meson masses, and the mean lifetime of mesons is not important and we ignore them in our analysis. In Table I and Table II, we present the most important theoretical and experimental inputs with their uncertainties that are used for our random scan.

We wish to study the effects of each new physics parameter on various observables and the $B_c \rightarrow \tau\nu$ and $B^0 \rightarrow \pi\tau\nu$ decays in a model independent way. We also consider the ratio of branching fractions of $B^0 \rightarrow \pi\tau\nu$ to $B^0 \rightarrow \pi l\nu$ decays, defined as

$$R_\pi = \frac{\mathcal{B}(B \rightarrow \pi\tau\nu)}{\mathcal{B}(B \rightarrow \pi l\nu)}, \tag{27}$$

which, in the SM, only depends on the ratio of form factors $F_0(q^2)/F_+(q^2)$. The decay mode $B \rightarrow \pi\tau\nu$ is particularly important because it originates from the same flavor changing interaction as the

CKM Elements:		Meson Decay constants (in GeV):	
$ V_{ub} $ (Exclusive)	$(3.23 \pm 0.31) \times 10^{-3}$ [5]	f_B	0.1906 ± 0.0047 [34–36]
$ V_{cb} $ (Average)	$(40.9 \pm 1.1) \times 10^{-3}$ [5]	f_{B_c}	0.395 ± 0.015 [37]
Inputs for $(B \rightarrow \pi)$ Form Factors:		Inputs for $(B \rightarrow D^*)$ Form Factors:	
$F_+(0) = F_0(0)$	0.281 ± 0.028 [27]	$h_{A_1}(1) V_{cb} $	$(34.6 \pm 1.02) \times 10^{-3}$ [39]
b_1	-1.62 ± 0.70 [27]	ρ_1^2	1.214 ± 0.035 [39]
b_1^0	-3.98 ± 0.97 [27]	$R_1(1)$	1.401 ± 0.038 [39]
Inputs for $(B \rightarrow D)$ Form Factors:		$R_2(1)$	0.864 ± 0.025 [39]
$V_1(1) V_{cb} $	$(43.0 \pm 2.36) \times 10^{-3}$ [38]	$R_0(1)$	1.14 ± 0.114 [14]
ρ_1^2	1.20 ± 0.098 [38]		

TABLE I: Theory input parameters

Ratio of branching ratios:	
R_π^l	0.73 ± 0.15 [12]
R_D	0.440 ± 0.072 [13]
R_{D^*}	0.332 ± 0.030 [13]

TABLE II: Experimental input parameters

$B \rightarrow \tau \nu$ decay mode and hence can be used as an indicator for NP operators. Similarly, the $B_c \rightarrow \tau \nu$ is important as it is mediated via $b \rightarrow c$ transition decays, same as $B \rightarrow D \tau \nu$ and $B \rightarrow D^* \tau \nu$ decays, and, in principle, can help in identifying the nature of NP in $b \rightarrow c$ processes. The SM prediction for the branching ratios and ratio of branching ratios is reported in Table. III, where, for the central values we have used the central values of all the input parameters from Eq. (26) and from Table. I. We vary all the theory inputs such as B_q meson decay constants, $B \rightarrow (P, V)$ transition form factors and the CKM matrix elements $|V_{qb}|$ within 1σ of their central values and obtain the 1σ allowed ranges in all the different observables in Table. III. The uncertainties associated with the

	Central value	1σ range
$\mathcal{B}(B \rightarrow \tau \nu)$	6.70×10^{-5}	$(5.22, 8.45) \times 10^{-5}$
$\mathcal{B}(B_c \rightarrow \tau \nu)$	1.63×10^{-2}	$(1.43, 1.85) \times 10^{-2}$
$\mathcal{B}(B \rightarrow \pi l \nu)$	12.77×10^{-5}	$(7.39, 21.28) \times 10^{-5}$
$\mathcal{B}(B \rightarrow \pi \tau \nu)$	8.91×10^{-5}	$(4.93, 15.40) \times 10^{-5}$
$\mathcal{B}(B \rightarrow D l \nu)$	2.32×10^{-2}	$(1.89, 2.81) \times 10^{-2}$
$\mathcal{B}(B \rightarrow D \tau \nu)$	0.72×10^{-2}	$(0.62, 0.84) \times 10^{-2}$
$\mathcal{B}(B \rightarrow D^* l \nu)$	4.93×10^{-2}	$(4.51, 5.39) \times 10^{-2}$
$\mathcal{B}(B \rightarrow D^* \tau \nu)$	1.25×10^{-2}	$(1.14, 1.37) \times 10^{-2}$
R_π^l	0.486	(0.328, 0.733)
R_π	0.698	(0.654, 0.764)
R_D	0.313	(0.300, 0.327)
R_D^*	0.253	(0.245, 0.261)

TABLE III: Branching ratio and ratio of branching ratios within the SM.

input parameters for the calculation of the form factors, reported in Appendix B and Appendix C, are added in quadrature and tabulated in Table I.

We now proceed to describe four different scenarios of new physics and the effect of these NP parameters. We consider all the NP parameters to be real for our analysis. We assume that only the third generation leptons get corrections from the NP couplings in the $b \rightarrow (u, c) l \nu$ processes and for $l = e^-, \mu^-$ cases the NP is absent. We use 3σ experimental constraint coming from the ratio of branching ratios R_π^l , R_D , and R_D^* to find the allowed ranges of all the NP couplings. We then show how different observables behave with various NP couplings under four different NP scenarios that we consider for our analysis. We also give predictions for the branching ratios of $B_c \rightarrow \tau \nu$ and $B \rightarrow \pi \tau \nu$ decays and the ratio R_π for all the different NP scenarios.

A. Scenario A

We vary V_L and V_R while keeping all other NP couplings to zero. The allowed ranges of V_L and V_R that satisfies 3σ constraint coming from R_π^l , R_D , and R_D^* are shown in the left panel of Fig. 1. We see that the experimental values put a severe constraint on the (V_L, V_R) parameter space. In

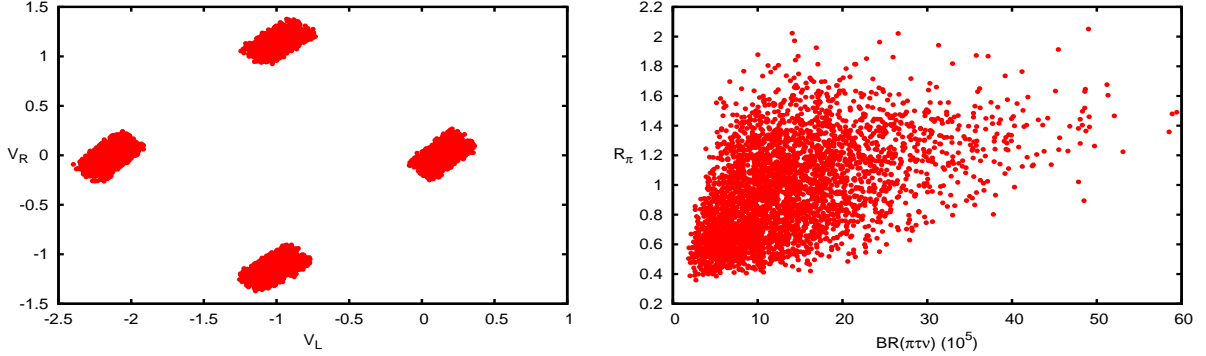


FIG. 1: Allowed regions of V_L and V_R are shown in the left panel once the 3σ experimental constraint is imposed. The corresponding ranges in $\mathcal{B}(B \rightarrow \pi\tau\nu)$ and the ratio R_π in the presence of these NP couplings are shown in the right panel.

the presence of such NP couplings, the $\Gamma(B_q \rightarrow \tau\nu)$, $d\Gamma/dq^2(B \rightarrow P\tau\nu)$, and $d\Gamma/dq^2(B \rightarrow V\tau\nu)$, where P stands for pseudoscalar and V stands for vector meson, can be written as

$$\begin{aligned} \Gamma(B_q \rightarrow \tau\nu) &= \Gamma(B_q \rightarrow \tau\nu)|_{\text{SM}} G_A^2, \\ \frac{d\Gamma}{dq^2}(B \rightarrow P\tau\nu) &= \left[\frac{d\Gamma}{dq^2}(B \rightarrow P\tau\nu) \right]_{\text{SM}} G_V^2, \\ \frac{d\Gamma}{dq^2}(B \rightarrow V\tau\nu) &= \frac{8 N |\vec{p}_V|}{3} \left\{ (\mathcal{A}_0^2 G_A^2 + \mathcal{A}_\parallel^2 G_A^2 + \mathcal{A}_\perp^2 G_V^2) \left(1 + \frac{m_\tau^2}{2q^2} \right) + \frac{3m_\tau^2}{2q^2} \mathcal{A}_t^2 G_A^2 \right\}. \end{aligned} \quad (28)$$

It is evident that, the value of $\mathcal{B}(B_c \rightarrow \tau\nu)$ varies as G_A^2 , whereas, $\mathcal{B}(B \rightarrow \pi\tau\nu)$ and the ratio R_π varies as G_V^2 in the presence of these NP couplings. The ranges in $B \rightarrow \pi\tau\nu$ branching ratio and the ratio R_π in the presence of V_L and V_R are shown in the right panel of Fig. 1. The resulting ranges in $\mathcal{B}(B_c \rightarrow \tau\nu)$, $\mathcal{B}(B \rightarrow \pi\tau\nu)$, and R_π are

$$\begin{aligned} \mathcal{B}(B_c \rightarrow \tau\nu) &= (1.02, 3.95)\%, & \mathcal{B}(B \rightarrow \pi\tau\nu) &= (1.86, 59.42) \times 10^{-5}, \\ R_\pi &= (0.36, 2.05). \end{aligned}$$

We see a significant deviation from the the SM expectation in such new physics scenario. Measurement of the $\mathcal{B}(B_c \rightarrow \tau\nu)$, $\mathcal{B}(B \rightarrow \pi\tau\nu)$ and the ratio R_π will put additional constraints on the NP parameters. We want to see the effects of these NP couplings on various observables that we defined

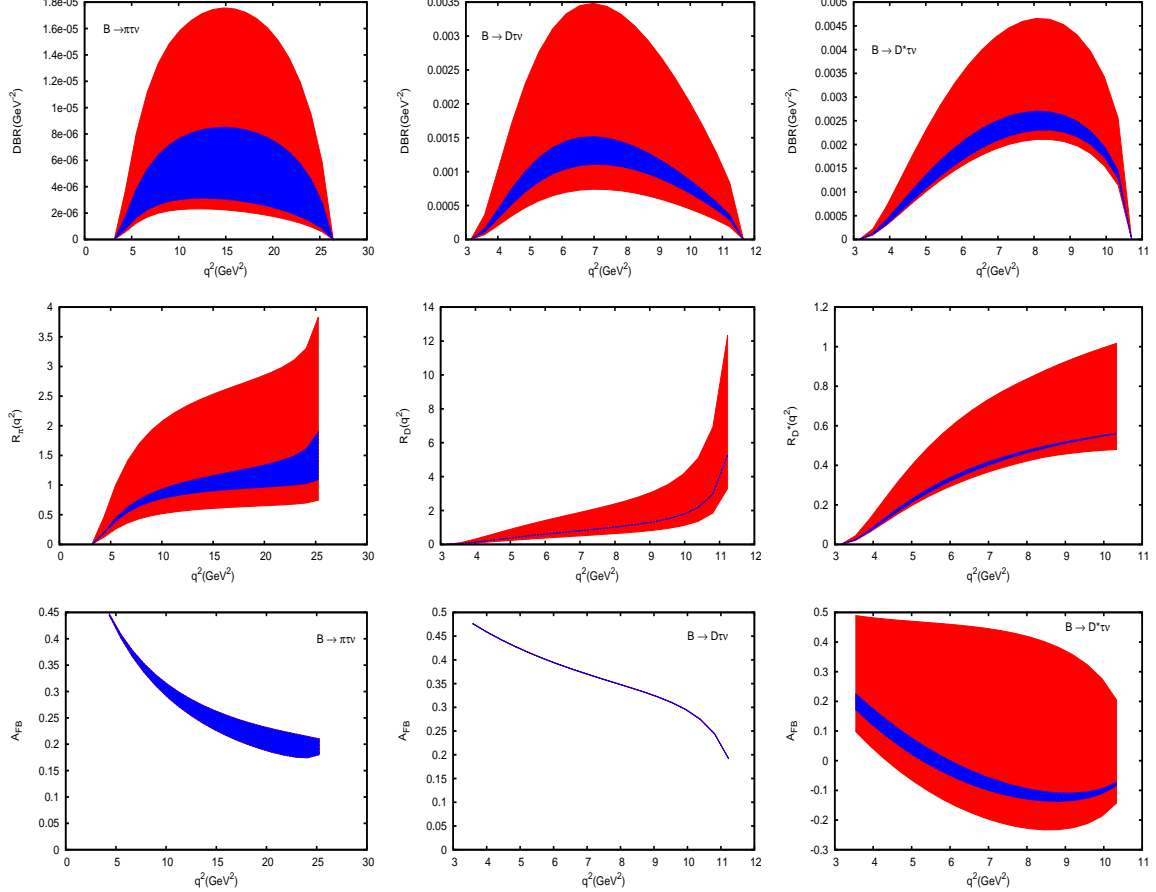


FIG. 2: Range in $\text{DBR}(q^2)$, $R(q^2)$, and the forward backward asymmetry $A_{FB}(q^2)$ for the $B \rightarrow \pi\tau\nu$, $B \rightarrow D\tau\nu$, and $B \rightarrow D^*\tau\nu$ decay modes. The darker (blue) interior region corresponds to the SM prediction, whereas, the lighter (red), larger region corresponds to the allowed (V_L, V_R) NP couplings of Fig. 1.

in Sec. II. In Fig. 2, we show in blue (dark) bands the SM range and show in red (light) bands the range of each observable once the NP couplings V_L and V_R are switched on. It is clear from Fig. 2 that, the differential branching ratios (DBR) and the ratio of branching ratio get considerable deviations once we include the NP couplings. This is expected and can be understood very easily from Eq. (28). In the presence of V_L and V_R alone, the DBR and the ratio for $B \rightarrow P\tau\nu$ decays

depends on only G_V coupling and is proportional to G_V^2 . Whereas, for $B \rightarrow V \tau \nu$ decay mode the DBR and the ratio depends on G_V as well as G_A couplings and is proportional to G_V^2 and G_A^2 as can be seen from Eq. (28). We see that the DBR for each decay mode can increase by 100% at the peak of its distribution. Similar conclusions can be made for the ratio of branching ratios as well where we see a 100% increase at the peak of its distribution. The forward-backward asymmetry, as we expected, does not vary with V_L and V_R for the $B \rightarrow \pi \tau \nu$ and the $B \rightarrow D \tau \nu$ decay modes. Since it depends on G_V couplings only, the NP dependency gets canceled in the ratio as can be seen from Eq. (22). However, for $B \rightarrow D^* \tau \nu$, the deviation is quite large. Again, it can be very easily understood from Eq. (24). It is mainly because of the presence of G_V as well as G_A couplings. We see a zero crossing at $q^2 \approx 6.0 \text{ GeV}^2$ in the SM for this decay mode. However, in the presence of such NP, depending on V_L and V_R , there may or may not be a zero crossing as is evident from Fig. 2.

Again, we want to emphasize the fact that a pure G_V coupling will contribute to the $B \rightarrow P \tau \nu$ as well as $B \rightarrow V \tau \nu$ decay processes, whereas a pure G_A coupling will contribute to the $B \rightarrow \tau \nu$ as well as the $B \rightarrow V \tau \nu$ decay modes. We do not consider pure G_V and G_A couplings for our analysis as a pure G_V or a pure G_A type NP coupling will not be able to accommodate all the existing data since current experiments on $b \rightarrow u$ and $b \rightarrow c$ semi-(leptonic) decays suggest that there could be new physics in all the three decay modes. Hence, if NP is present in R_π^l , R_D , and R_{D^*} , one can rule out the possibility of having a pure G_V or a pure G_A type of NP couplings.

B. Scenario B

Here we consider nonzero S_L and S_R couplings and keep all other NP couplings to zero. The allowed ranges of S_L and S_R that satisfy the 3σ experimental constraints are shown in the left panel of Fig. 3. In the presence of S_L and S_R , the $\Gamma(B_q \rightarrow \tau \nu)$, $d\Gamma/dq^2(B \rightarrow P \tau \nu)$, and $d\Gamma/dq^2(B \rightarrow V \tau \nu)$ can be written as

$$\begin{aligned}\Gamma(B_q \rightarrow \tau \nu) &= \Gamma(B_q \rightarrow \tau \nu)|_{\text{SM}} \left[1 - \frac{m_B^2}{m_\tau(m_b + m_q)} G_P \right]^2, \\ \frac{d\Gamma}{dq^2}(B \rightarrow P \tau \nu) &= \frac{8N|\vec{p}_P|}{3} \left\{ H_0^2 \left(1 + \frac{m_\tau^2}{2q^2} \right) + \frac{3m_\tau^2}{2q^2} H_t^2 + \frac{3}{2} \left(H_S^2 G_S^2 + \frac{2m_\tau}{\sqrt{q^2}} H_t H_S G_S \right) \right\}, \\ \frac{d\Gamma}{dq^2}(B \rightarrow V \tau \nu) &= \frac{8N|\vec{p}_V|}{3} \left\{ (\mathcal{A}_0^2 + \mathcal{A}_\parallel^2 + \mathcal{A}_\perp^2) \left(1 + \frac{m_\tau^2}{2q^2} \right) + \frac{3m_\tau^2}{2q^2} \mathcal{A}_t^2 \right.\end{aligned}$$

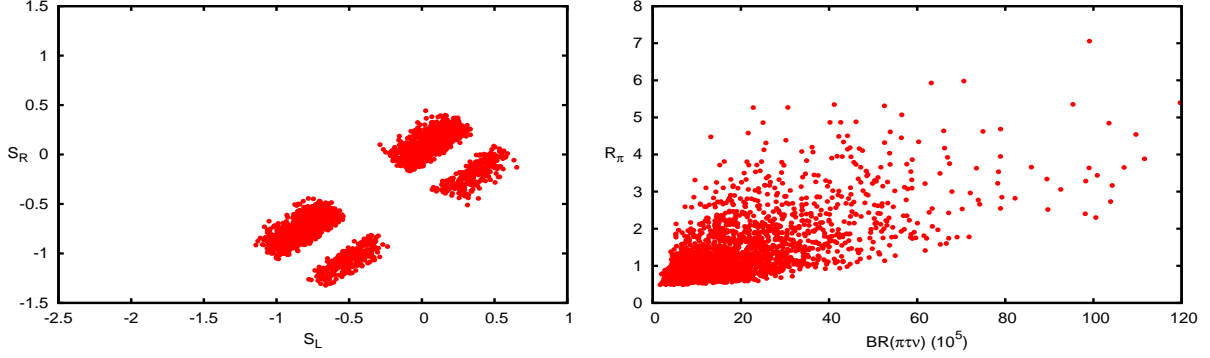


FIG. 3: Allowed ranges of (S_L, S_R) is shown in the left panel once the experimental constraint is imposed. The right panel shows the ranges of $B \rightarrow \pi\tau\nu$ branching fractions and the ratio R_π with these NP couplings.

$$+ \frac{3}{2} \left(\mathcal{A}_P^2 G_P^2 + \frac{2m_\tau}{\sqrt{q^2}} \mathcal{A}_t \mathcal{A}_P G_P \right) \Big\} \quad (29)$$

We see that $B \rightarrow \tau\nu$ and $B \rightarrow D^*\tau\nu$ depend on pure G_P coupling, whereas, $B \rightarrow \pi\tau\nu$ and $B \rightarrow D\tau\nu$ depend on pure G_S coupling. Hence, we do not consider pure G_P and pure G_S NP couplings for our analysis as these will not simultaneously explain all the existing data. The effects of these NP couplings on the $\mathcal{B}(B \rightarrow \pi\tau\nu)$ and the ratio R_π is shown in the right panel of Fig. 3. In the presence of such NP, the 3σ allowed ranges of the branching ratio of $B_c \rightarrow \tau\nu$, $B \rightarrow \pi\tau\nu$, and the ratio R_π of the branching ratios of $B \rightarrow \pi\tau\nu$ to the corresponding $B \rightarrow \pi l \nu$ are

$$\begin{aligned} \mathcal{B}(B_c \rightarrow \tau\nu) &= (0.21, 13.66)\%, & \mathcal{B}(B \rightarrow \pi\tau\nu) &= (1.69, 119.66) \times 10^{-5}, \\ R_\pi &= (0.49, 7.06). \end{aligned}$$

We see that the $\mathcal{B}(B_c \rightarrow \tau\nu)$, $\mathcal{B}(B \rightarrow \pi\tau\nu)$, and the ratio R_π are quite sensitive to the S_L and S_R NP couplings. The deviation from the SM is quite large once these NP couplings are switched on.

We now wish to see how different observables behave with S_L and S_R . The corresponding DBR, the ratio $R(q^2)$, and the forward-backward asymmetries $A_{FB}(q^2)$ as a function of q^2 are shown in Fig. 4. We see that deviation from the SM is much larger in the case of $B \rightarrow \pi\tau\nu$ and $B \rightarrow D\tau\nu$ decay modes than the $B \rightarrow D^*\tau\nu$ decay mode. We see that the variation is quite similar in $B \rightarrow \pi\tau\nu$ and $B \rightarrow D\tau\nu$ decay modes. It is expected as both the decay modes depend on the NP couplings through G_S , whereas the $B \rightarrow D^*\tau\nu$ depends on the NP couplings through G_P and hence the variation is quite different from the $B \rightarrow \pi\tau\nu$ and $B \rightarrow D\tau\nu$ decay modes. Again, the peak of the

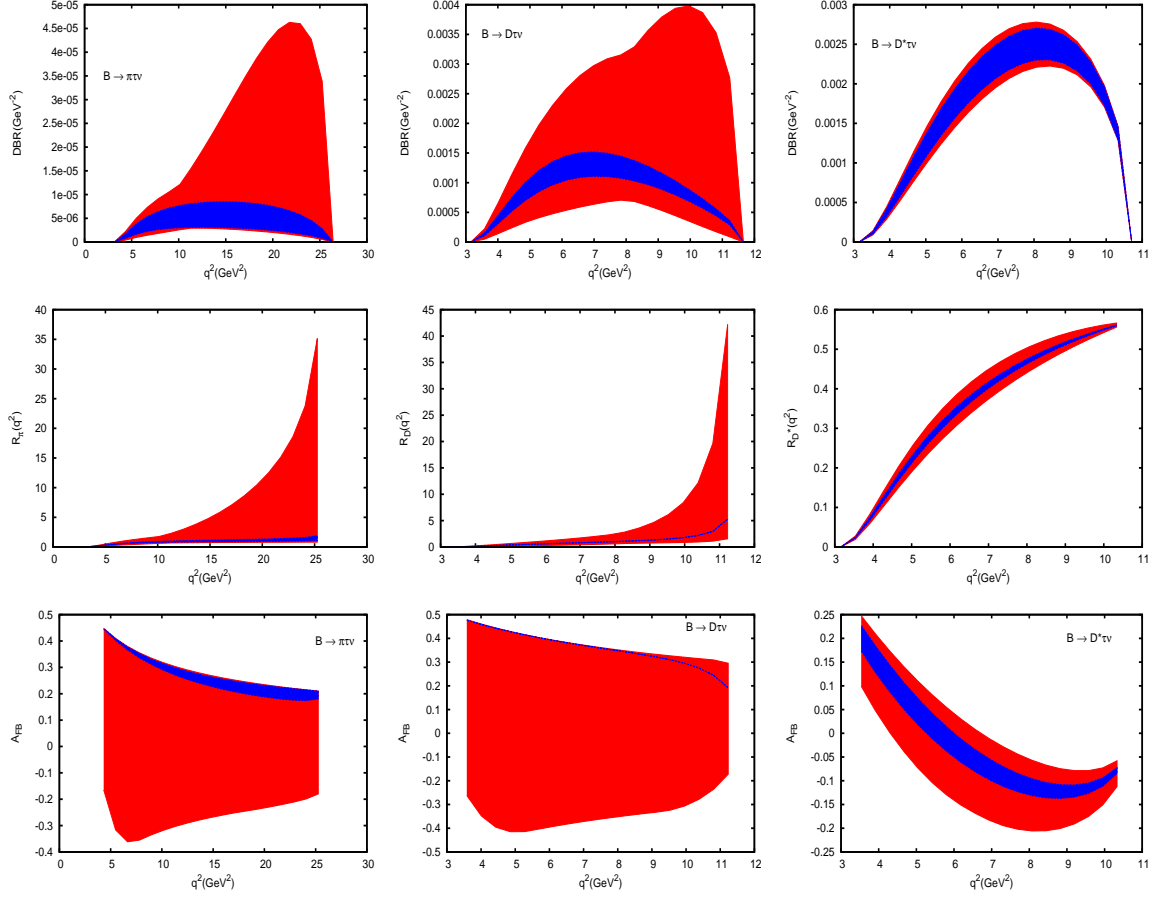


FIG. 4: Range in $\text{DBR}(q^2)$, $R(q^2)$, and the forward-backward asymmetry $A_{FB}(q^2)$ for the $B \rightarrow \pi\tau\nu$, $B \rightarrow D\tau\nu$, and $B \rightarrow D^*\tau\nu$ decay modes. The darker (blue) interior region corresponds to the SM prediction, whereas, the lighter (red), larger region corresponds to the allowed (S_L, S_R) NP couplings of Fig. 3.

distribution of differential branching ratio for the $B \rightarrow \pi\tau\nu$ and $B \rightarrow D\tau\nu$ can shift to a higher q^2 region once the NP couplings are introduced.

Again in the SM, as mentioned earlier, we see a zero crossing in the forward-backward asymmetry for the $B \rightarrow D^*\tau\nu$ decay mode. Moreover, we observe no such zero crossing in case of $B \rightarrow \pi\tau\nu$ and $B \rightarrow D\tau\nu$ decay modes. However, once the NP couplings S_L and S_R are switched on, we see a zero crossing for the $B \rightarrow \pi\tau\nu$ as well as the $B \rightarrow D\tau\nu$ decay modes. Depending on the value of the NP couplings, there may be a zero crossing or there could be a total change of sign of the A_{FB} parameter as can be seen from Fig. 4. Thus, we see that, the forward-backward asymmetry

in the case of $B \rightarrow \pi\tau\nu$ and $B \rightarrow D\tau\nu$ is very sensitive to the S_L and S_R couplings. In the case of $B \rightarrow D^*\tau\nu$ decay mode, however, the sensitivity is much smaller than the $B \rightarrow \pi\tau\nu$ and $B \rightarrow D\tau\nu$ modes. It is worth mentioning that, depending on the value of the NP couplings, there can be a zero crossing for the $B \rightarrow D^*\tau\nu$ decay process which is marginally different from the SM, as is evident from Fig. 4.

C. Scenario C

We set all the other NP couplings to zero while varying \tilde{V}_L and \tilde{V}_R . These couplings are related to the right-handed neutrino interactions. As already mentioned in Sec. II, the decay rate depends quadratically on these NP couplings. The linear term that comes from the interference between the SM and the NP is negligible due to the mass of the neutrino. The allowed ranges of \tilde{V}_L and \tilde{V}_R are shown in the left panel of Fig. 5. It is evident that the parameter space is much less restricted than Scenario A ($V_{L,R} \neq 0$) and Scenario B ($S_{L,R} \neq 0$).

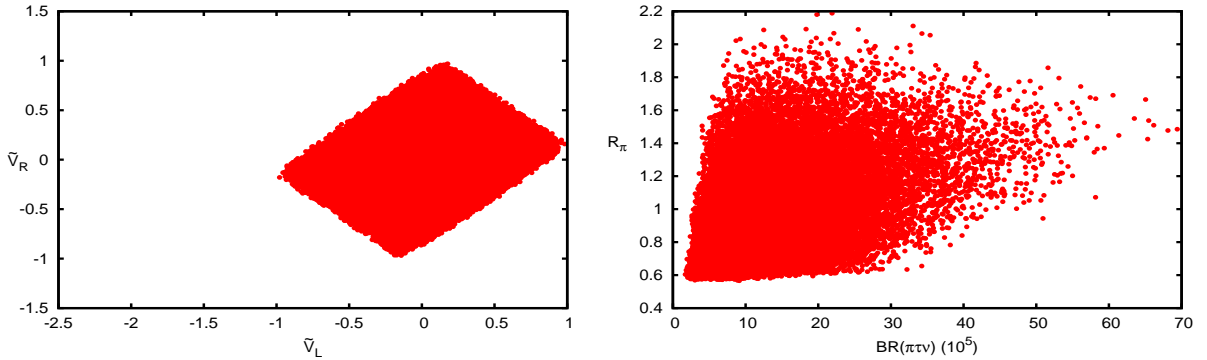


FIG. 5: Range in \tilde{V}_L and \tilde{V}_R is shown in the left panel once the 3σ experimental constraint is imposed. The resulting range in the $\mathcal{B}(B \rightarrow \pi\tau\nu)$ and R_π is shown in the right panel with these NP couplings.

In the presence of such NP couplings, the $\Gamma(B_q \rightarrow \tau\nu)$, $d\Gamma/dq^2(B \rightarrow P\tau\nu)$, and $d\Gamma/dq^2(B \rightarrow V\tau\nu)$, where P stands for pseudoscalar and V stands for vector meson, can be written as

$$\begin{aligned}\Gamma(B_q \rightarrow \tau\nu) &= \Gamma(B_q \rightarrow \tau\nu)|_{\text{SM}} \left(1 + \tilde{G}_A^2\right), \\ \frac{d\Gamma}{dq^2}(B \rightarrow P\tau\nu) &= \left(\frac{d\Gamma}{dq^2}(B \rightarrow P\tau\nu)\right)_{\text{SM}} \left(1 + \tilde{G}_V^2\right), \\ \frac{d\Gamma}{dq^2}(B \rightarrow V\tau\nu) &= \frac{8N|\vec{p}_V|}{3} \left\{ \left[\mathcal{A}_0^2(1 + \tilde{G}_A^2) + \mathcal{A}_\parallel^2(1 + \tilde{G}_A^2) + \mathcal{A}_\perp^2(1 + \tilde{G}_V^2) \right] \left(1 + \frac{m_\tau^2}{2q^2}\right) \right\}\end{aligned}$$

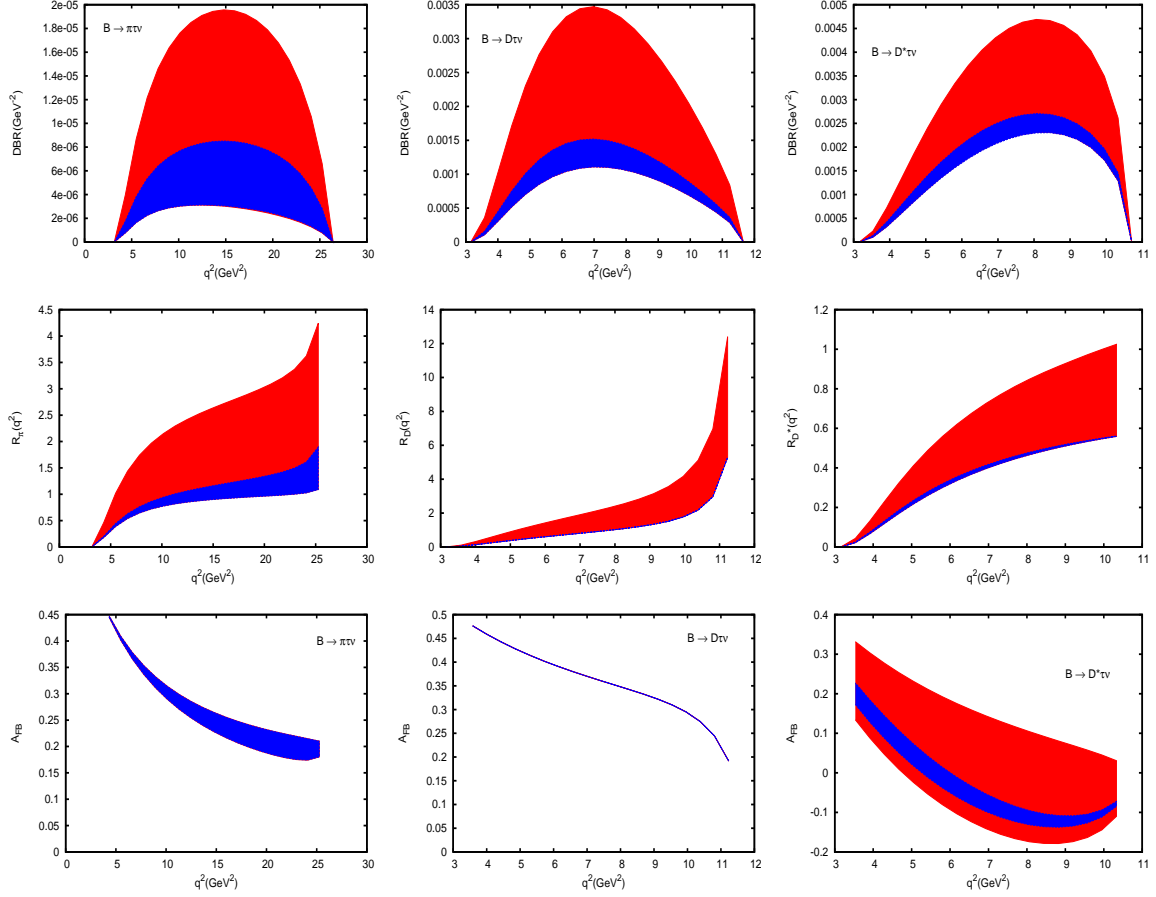


FIG. 6: Range in $\text{DBR}(q^2)$, $R(q^2)$, and $A_{FB}(q^2)$ for the $B \rightarrow \pi\tau\nu$, $B \rightarrow D\tau\nu$, and the $B \rightarrow D^*\tau\nu$ decay modes. The dark (blue) band corresponds to the SM range, whereas, the light (red) band corresponds to the NP couplings (\tilde{V}_L , \tilde{V}_R) that are shown in the left panel of Fig. 5.

$$\left. + \frac{3m_\tau^2}{2q^2} \mathcal{A}_t^2 (1 + \tilde{G}_A^2) \right\} \quad (30)$$

It is evident from Eq. (30) that the $B \rightarrow \tau\nu$ decay branching ratio depends on the NP couplings through \tilde{G}_A^2 term and the $B \rightarrow D^*\tau\nu$ branching ratio depend on \tilde{V}_L and \tilde{V}_R couplings through \tilde{G}_A^2 as well as \tilde{G}_V^2 term, whereas the $B \rightarrow \pi\tau\nu$ and $B \rightarrow D\tau\nu$ branching ratios depend on these couplings through \tilde{G}_V^2 term. The corresponding 3σ allowed ranges of $\mathcal{B}(B \rightarrow \pi\tau\nu)$ and the ratio R_π is shown in the right panel of Fig. 5. The ranges are

$$\begin{aligned} \mathcal{B}(B_c \rightarrow \tau\nu) &= (1.09, 4.13)\%, & \mathcal{B}(B \rightarrow \pi\tau\nu) &= (1.71, 69.39) \times 10^{-5}, \\ R_\pi &= (0.57, 2.19), \end{aligned}$$

and are quite similar to Scenario A. Again, a significant deviation from the SM prediction is expected in such NP scenario.

The allowed ranges of all the different observables with these NP couplings are shown in Fig. 6. We see that the differential branching ratio, the ratio of branching ratio, and the forward backward asymmetry parameters vary quite significantly with the inclusion of the NP couplings. The q^2 distribution looks quite similar to what we obtain for Scenario A. Although, the differential branching ratio and the ratio of branching ratios are quite sensitive to \tilde{V}_L and \tilde{V}_R , the forward-backward asymmetry for the $B \rightarrow \pi\tau\nu$ and $B \rightarrow D\tau\nu$ does not depend on the NP couplings at all. However, for the $B \rightarrow D^*\tau\nu$ decay mode, all the three observables are very sensitive to these right-handed neutrino couplings. Again, depending on these NP couplings, there may be a zero crossing in the q^2 distribution of the A_{FB} parameter which can be quite different from the SM prediction.

D. Scenario D

We include the new physics effects coming from the \tilde{S}_L and \tilde{S}_R alone while keeping all the other NP couplings to zero. We impose the experimental constraint coming from the measured data of R_π^l , R_D , and R_{D^*} and the resulting allowed ranges of \tilde{S}_L and \tilde{S}_R are shown in the left panel of Fig. 7. Similar to \tilde{V}_L and \tilde{V}_R , these couplings also arise due to the right-handed neutrino interactions. The decay rate depends on these NP couplings quadratically and hence the parameter space is less constrained. In the presence of \tilde{S}_L and \tilde{S}_R , the $\Gamma(B_q \rightarrow \tau\nu)$, $d\Gamma/dq^2(B \rightarrow P\tau\nu)$, and $d\Gamma/dq^2(B \rightarrow V\tau\nu)$ can be written as

$$\begin{aligned}\Gamma(B_q \rightarrow \tau\nu) &= \Gamma(B_q \rightarrow \tau\nu)|_{\text{SM}} \left[1 + \frac{m_B^4}{m_\tau^2 (m_b + m_q)^2} \tilde{G}_P^2 \right], \\ \frac{d\Gamma}{dq^2}(B \rightarrow P\tau\nu) &= \frac{8N|\vec{p}_P|}{3} \left\{ H_0^2 \left(1 + \frac{m_\tau^2}{2q^2} \right) + \frac{3m_\tau^2}{2q^2} H_t^2 + \frac{3}{2} H_S^2 \tilde{G}_S^2 \right\}, \\ \frac{d\Gamma}{dq^2}(B \rightarrow V\tau\nu) &= \frac{8N|\vec{p}_V|}{3} \left\{ (\mathcal{A}_0^2 + \mathcal{A}_\parallel^2 + \mathcal{A}_\perp^2) \left(1 + \frac{m_\tau^2}{2q^2} \right) + \frac{3m_\tau^2}{2q^2} \mathcal{A}_t^2 + \frac{3}{2} \mathcal{A}_P^2 \tilde{G}_P^2 \right\}.\end{aligned}\quad (31)$$

The 3σ allowed ranges of the $B \rightarrow \pi\tau\nu$ branching ratio and the ratio R_π are shown in the right panel of Fig. 7. The ranges of $\mathcal{B}(B_c \rightarrow \tau\nu)$, $\mathcal{B}(B \rightarrow \pi\tau\nu)$, and R_π are

$$\begin{aligned}\mathcal{B}(B_c \rightarrow \tau\nu) &= (1.11, 16.71)\%, & \mathcal{B}(B \rightarrow \pi\tau\nu) &= (1.70, 93.90) \times 10^{-5}, \\ R_\pi &= (0.56, 4.32).\end{aligned}$$

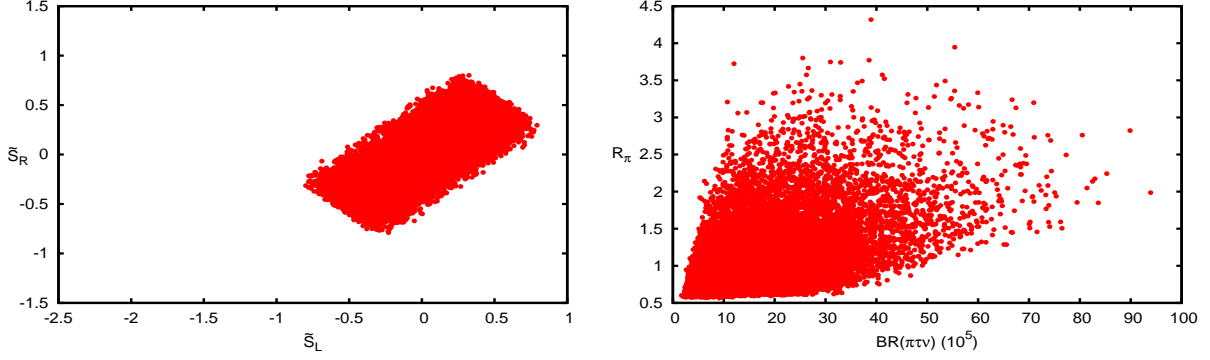


FIG. 7: Left panel shows the allowed range in \tilde{S}_L and \tilde{S}_R with the 3σ experimental constraint imposed. The resulting range in $B \rightarrow \pi\tau\nu$ branching ratio and the ratio R_π is shown in the right panel once the NP \tilde{S}_L and \tilde{S}_R are included.

The effect of these NP couplings on various observables are quite similar to the scenario where only the S_L and S_R are nonzero. The allowed ranges of all the observables are shown in Fig. 8. The differential branching ratio, the ratio of branching ratios, and the forward-backward asymmetry parameters deviate quite significantly from the SM prediction for the $B \rightarrow \pi\tau\nu$ and $B \rightarrow D\tau\nu$ decay modes, whereas there is no or very little deviation of these observables from the SM value in case of $B \rightarrow D^*\tau\nu$ decay process. We see that the $B \rightarrow \tau\nu$ and $B \rightarrow D^*\tau\nu$ decay branching ratios depend on these NP couplings through \tilde{G}_P^2 terms, but, the $B \rightarrow \pi\tau\nu$ and $B \rightarrow D\tau\nu$ decay branching fractions depend on these NP couplings through \tilde{G}_S^2 terms. Hence, we see similar behavior for the $B \rightarrow \pi\tau\nu$ and $B \rightarrow D\tau\nu$ decay modes. However, as expected, the variation in the $B \rightarrow D^*\tau\nu$ decay mode is quite different from the $B \rightarrow \pi\tau\nu$ and the $B \rightarrow D\tau\nu$ decay modes. Again, we see that the peak of the distribution of $B \rightarrow \pi\tau\nu$ and $B \rightarrow D\tau\nu$ decay branching ratios shift toward a large q^2 region. Although, the effects of these right-handed couplings are quite similar to its left-handed counterpart, there are some differences. We do not see any zero crossing in the q^2 distribution of the A_{FB} parameter for the $B \rightarrow \pi\tau\nu$ and $B \rightarrow D\tau\nu$ decay modes.

IV. CONCLUSION

B decay measurements have been providing us a lot of useful information regarding the nature of new physics. Several recent measurements in the rare processes have put severe constraints

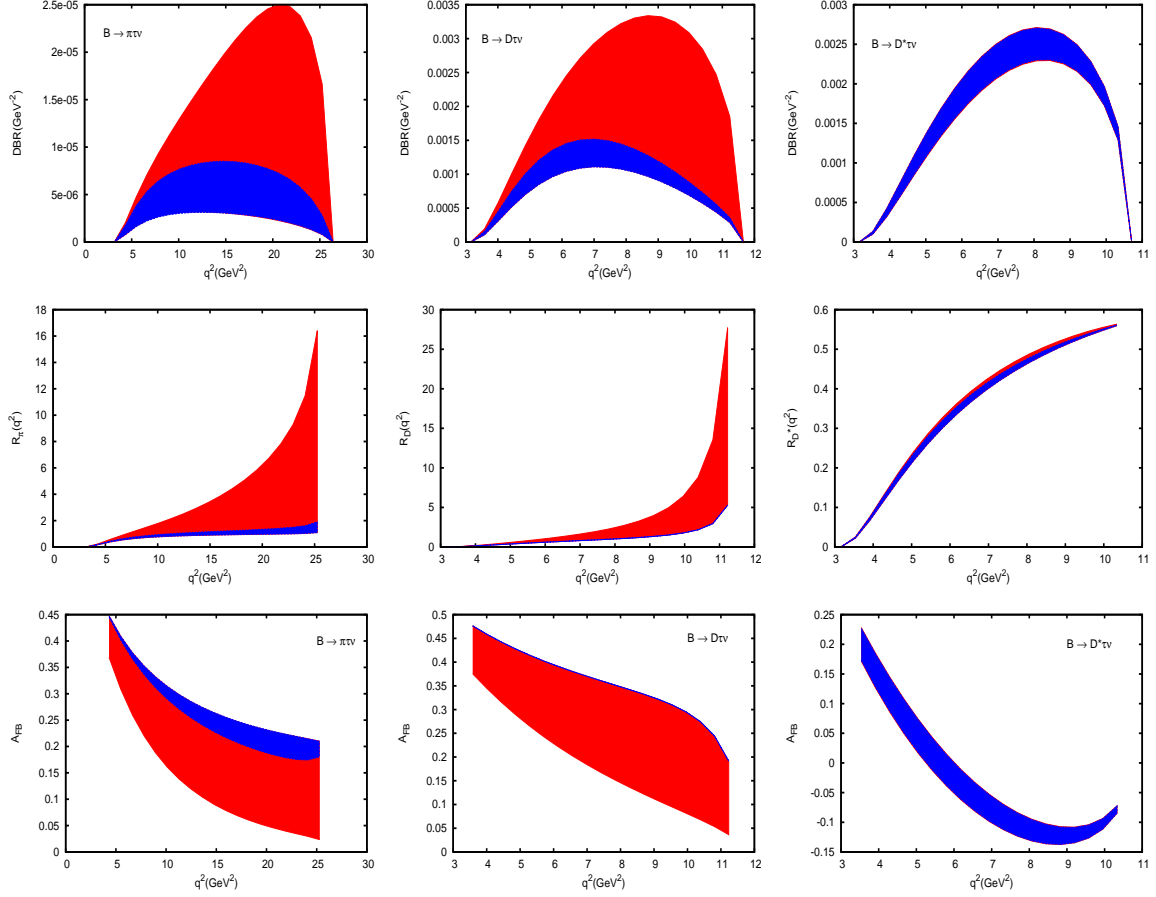


FIG. 8: Range in various observables such as $\text{DBR}(q^2)$, $R(q^2)$, and $A_{FB}(q^2)$ for the $B \rightarrow \pi \tau \nu$, $B \rightarrow D \tau \nu$, and the $B \rightarrow D^* \tau \nu$ decays. The allowed range in each observable is shown in light (red) band once the NP couplings $(\tilde{S}_L, \tilde{S}_R)$ are varied within the allowed ranges as shown in the left panel of Fig. 7. The corresponding SM prediction is shown in dark (blue) band.

on the NP parameters. Precision measurements in B meson decays have been a great platform for indirect evidences of beyond the standard model physics. The recent measurements of the ratio of the branching ratio R_D of $B \rightarrow D \tau \nu$ to that of $B \rightarrow D l \nu$ and R_D^* of $B \rightarrow D^* \tau \nu$ to that of $B \rightarrow D^* l \nu$ differ from the standard model expectation at the 3.4σ level. It is still not conclusive enough that new physics is indeed present in this $b \rightarrow c \tau \nu$ processes. More precise measurements will reveal the nature of the new physics. Similar new physics effects have been observed in $b \rightarrow u \tau \nu$ processes as well. The measurement of the branching ratio of $B \rightarrow \tau \nu$ and the ratio R_π^l of the branching ratio of $B \rightarrow \tau \nu$ to $B \rightarrow \pi l \nu$ decays differ from the standard

model expectation at more than the 2.5σ level. A lot of phenomenological studies have been done in order to explain all these discrepancies. In this paper, we consider an effective Lagrangian for the $b \rightarrow q l \nu$ transition processes in the presence of NP, where $q = u, c$, and perform a combined analysis of $B \rightarrow \tau \nu$, $B \rightarrow D \tau \nu$ and $B \rightarrow D^* \tau \nu$ decay processes. Our work differs significantly from others as we include the right-handed neutrino couplings. We assume that new physics is present only in the third generation leptons. We look at four different new physics scenarios. The results of our analysis are as follows.

We assume new physics in the third generation lepton only and see the effect of each new physics couplings on various observables. We first find the allowed ranges of each NP coupling using a 3σ constraint coming from the most recent data of R_π^l , R_D , and R_{D^*} . For nonzero V_L and V_R couplings, the differential branching ratio and the ratio of branching ratios are quite sensitive to these NP couplings for each decay mode. However, the forward-backward asymmetry for the $B \rightarrow \pi \tau \nu$ and $B \rightarrow D \tau \nu$ is not sensitive to these couplings at all. The forward-backward asymmetry is quite sensitive to these NP couplings for $B \rightarrow D^* \tau \nu$ decays and the deviation from the standard model prediction can be quite significant depending on the value of V_L and V_R . Although, we see a zero crossing in the q^2 distribution, it may or may not be there depending on the NP couplings. Again, even if we see a zero crossing, it can deviate quite significantly from the standard model prediction.

In the case of S_L and S_R couplings, all the observables such as the differential branching ratio, ratio of branching ratios, and the forward-backward asymmetry are quite sensitive to the NP couplings for the $B \rightarrow \pi \tau \nu$ and $B \rightarrow D \tau \nu$ decays. However, the sensitivity is somewhat reduced for the $B \rightarrow D^* \tau \nu$ decay mode. Although, in the standard model, there is no zero crossing in the forward-backward asymmetry parameter for the $B \rightarrow \pi \tau \nu$ and $B \rightarrow D \tau \nu$ decay modes, however, depending on the value of S_L and S_R , one might see a zero crossing for both the decay modes. For the $B \rightarrow D^* \tau \nu$ mode, the zero crossing can be similar or marginally different from the standard model one.

For the right-handed neutrino couplings $(\tilde{V}_L, \tilde{V}_R)$ and $(\tilde{S}_L, \tilde{S}_R)$, the effects are quite similar to its left-handed counterpart (V_L, V_R) and (S_L, S_R) . However, the sensitivity is somewhat reduced.

Although current experimental results are pointing towards the third generation leptons for possible new physics, there could be, in principle, new physics in the first two generations as well. If there is NP in all generation leptons, then it might be possible to identify it by measuring the forward-backward asymmetry for $B \rightarrow \pi l \nu$, $B \rightarrow D l \nu$, and $B \rightarrow D^* l \nu$ decay modes, where

l could be either an electron or a muon. It will provide useful information regarding the NP couplings (S_L, S_R) and $(\tilde{S}_L, \tilde{S}_R)$. Similarly, measurement of the branching ratio of $B_c \rightarrow \tau \nu$ and $B \rightarrow \pi \tau \nu$ and the ratio R_π will put additional constraints on the nature of NP couplings. Retaining our current approach, we could also sharpen our estimates once improved measurements of various branching ratios and the ratio of branching ratios become available. At the same time, reducing the theoretical uncertainties in various form factors and decay constants will also improve our estimates in future.

Acknowledgments

R. D. and A. K. G. would like to thank BRNS, Government of India for financial support.

Appendix A: Kinematics and Helicity Amplitudes

We use the helicity method of Refs. [31, 32] to calculate the different helicity amplitudes for a B meson decaying to pseudoscalar(vector) meson along with a charged lepton and an antineutrino in the final state. We know that the amplitude square of the decay $B \rightarrow P(V) l \nu$ can be factorised into leptonic ($L_{\mu\nu}$) and hadronic ($H_{\mu\nu}$) tensors. That is

$$|\mathcal{M}(B \rightarrow P(V) l \nu)|^2 = |\langle P(V) l \nu | \mathcal{L}_{\text{eff}} | B \rangle|^2 = L_{\mu\nu} H^{\mu\nu}. \quad (\text{A1})$$

The leptonic and hadronic tensor product $L_{\mu\nu} H^{\mu\nu}$ depends on the polar angle $\cos \theta_l$, where θ_l is the angle between the P (V) meson three momentum vector and the lepton three momentum vector in the q^2 rest frame, and can be worked out using the completeness relation of the polarization four vectors $\epsilon(t, \pm, 0)$, i.e,

$$\sum_{m, m'=\pm, 0} \epsilon^\mu(m) \epsilon^{*\nu}(m') g_{mm'} = g^{\mu\nu}, \quad (\text{A2})$$

where $g_{mm'} = \text{diag}(+, -, -, -)$. Using this approach, one can factorize $L_{\mu\nu} H^{\mu\nu}$ in terms of two Lorentz invariant quantities such that

$$\begin{aligned} L_{\mu\nu} H^{\mu\nu} &= L^{\mu'\nu'} g_{\mu'\mu} g_{\nu'\nu} H^{\mu\nu} = \sum_{m, m', n, n'} L^{\mu'\nu'} \epsilon_{\mu'}(m) \epsilon_\mu^*(m') g_{mm'} \epsilon_{\nu'}^*(n) \epsilon_\nu(n') g_{nn'} H^{\mu\nu} \\ &= \sum_{m, m', n, n'} \left(L^{\mu'\nu'} \epsilon_{\mu'}(m) \epsilon_{\nu'}^*(n) \right) \left(H^{\mu\nu} \epsilon_\mu^*(m') \epsilon_\nu(n') \right) g_{mm'} g_{nn'} \end{aligned}$$

$$= \sum_{m, m', n, n'} L(m, n) H(m', n') g_{m m'} g_{n n'}, \quad (\text{A3})$$

where $L(m, n)$ and $H(m', n')$ can now be evaluated in different Lorentz frames. We evaluate $L(m, n)$ in the $l - \nu$ center-of-mass frame, i.e, in the q^2 rest frame and $H(m', n')$ in the B meson rest frame.

In the B meson rest frame, the helicity basis ϵ is taken to be

$$\begin{aligned} \epsilon(0) &= \frac{1}{\sqrt{q^2}}(|p_M|, 0, 0, -q_0), & \epsilon(\pm) &= \pm \frac{1}{\sqrt{2}}(0, \pm 1, -i, 0), \\ \epsilon(t) &= \frac{1}{\sqrt{q^2}}(q_0, 0, 0, -|p_M|), \end{aligned} \quad (\text{A4})$$

where $q_0 = (m_B^2 - m_M^2 + q^2)/2m_B$ and $q = p_B - p_M$ is the momentum transfer, respectively. Here m_M and p_M denote the mass and the four momentum of the final state pseudoscalar(vector) meson M , respectively. Again, we have $|p_M| = \lambda^{1/2}(m_B^2, m_M^2, q^2)/2m_B$. In the B meson rest frame, the B and M meson four momenta p_B and p_M are

$$p_B = (m_B, 0, 0, 0), \quad p_M = (E_M, 0, 0, |\vec{p}_M|), \quad (\text{A5})$$

where the $E_M = (m_B^2 + m_M^2 - q^2)/2m_B$. For a vector meson in the final state, the polarization four vectors obey the following orthonormality condition

$$\epsilon_\alpha^*(m) \epsilon^\alpha(m') = -\delta_{mm'} \quad (\text{A6})$$

and the completeness relation

$$\sum_{m, m'} \epsilon_\alpha(m) \epsilon_\beta(m') \delta_{mm'} = -g_{\alpha\beta} + \frac{(p_V)_\alpha (p_V)_\beta}{m_V^2}. \quad (\text{A7})$$

The leptonic tensor $L(m, n)$ is evaluated in the $l - \nu_l$ center-of-mass frame, i.e, in the q^2 rest frame. In this frame, the helicity basis ϵ is taken to be

$$\epsilon(0) = (0, 0, 0, -1), \quad \epsilon(\pm) = \pm \frac{1}{\sqrt{2}}(0, \pm 1, -i, 0), \quad \epsilon(t) = (1, 0, 0, 0) \quad (\text{A8})$$

In the q^2 rest frame, the four momenta of the lepton and the antineutrino pair can be written as

$$\begin{aligned} p_l^\mu &= (E_l, |p_l| \sin \theta_l, 0, -|p_l| \cos \theta_l), \\ p_\nu^\mu &= (|p_l|, -|p_l| \sin \theta_l, 0, |p_l| \cos \theta_l), \end{aligned} \quad (\text{A9})$$

where the lepton energy $E_l = (q^2 + m_l^2)/2\sqrt{q^2}$ and the magnitude of its three momenta is $|p_l| = (q^2 - m_l^2)/2\sqrt{q^2}$.

Appendix B: B to π Form Factors

For the $B \rightarrow \pi$ transition form factors, there are two nonperturbative methods for calculating the $B \rightarrow \pi$ form factors: light-cone sum rules (LCSR) and lattice QCD (LQCD). QCD light-cone sum rules with pion distribution amplitudes allow one to calculate the $B \rightarrow \pi$ form factors at small and intermediate momentum transfers $0 \leq q^2 \leq q_{\text{max}}^2$, where q_{max}^2 varies from 12 to 16 GeV² [40]. The most recent lattice QCD computations with three dynamical flavors predict these form factors at $q^2 \geq 16 \text{ GeV}^2$, in the upper part of the semileptonic region $0 \leq q^2 \leq (m_B - m_\pi)^2$, with an accuracy reaching 10%. There are also recent results available in the quenched approximation on a fine lattice [41]. Very recently, in Ref. [27], the author uses the sum rule results for the form factors as an input for a z-series parametrization that yield the q^2 shape in the whole semileptonic region of $B \rightarrow \pi l \nu$. The relevant formulae for $F_+(q^2)$ and $F_0(q^2)$ pertinent for our discussion, taken from Ref. [27], are

$$\begin{aligned} F_+(q^2) &= \frac{F_+(0)}{\left(1 - \frac{q^2}{m_B^2}\right)} \left\{ 1 + \sum_{k=1}^{N-1} b_k \left(z(q^2, t_0)^k - z(0, t_0)^k - (-1)^{N-k} \frac{k}{N} \left[z(q^2, t_0)^N - z(0, t_0)^N \right] \right) \right\} \\ F_0(q^2) &= F_0(0) \left\{ 1 + \sum_{k=1}^N b_k^0 \left(z(q^2, t_0)^k - z(0, t_0)^k \right) \right\} \end{aligned} \quad (\text{B1})$$

where by default $F_+(0) = F_0(0)$ and

$$z(q^2, t_0) = \frac{\sqrt{(m_B + m_\pi)^2 - q^2} - \sqrt{(m_B + m_\pi)^2 - t_0}}{\sqrt{(m_B + m_\pi)^2 - q^2} + \sqrt{(m_B + m_\pi)^2 - t_0}} \quad (\text{B2})$$

where the auxiliary parameter t_0 is defined as $t_0 = (m_B + m_\pi)^2 - 2\sqrt{m_B m_\pi} \sqrt{(m_B + m_\pi)^2 - q_{\text{min}}^2}$. The central values of $F_+(0) = F_0(0)$ and the slope parameters b_1 and b_1^0 are

$$F_0(0) = F_+(0) = 0.281 \pm 0.028, \quad b_1 = -1.62 \pm 0.70, \quad b_1^0 = -3.98 \pm 0.97 \quad (\text{B3})$$

For the uncertainties, we add the various errors reported in Ref. [27] in quadrature.

Appendix C: $B \rightarrow D, D^*$ form Factors using HQET

In the heavy quark effective theory one can write the hadronic matrix elements of current between two hadrons in inverse powers of heavy quark mass and the hadronic form factor in a reduced single universal form, which is a function of the kinematic variable $v_B \cdot v_{P(V)}$, where v_B and $v_{P(V)}$ are the

four velocity of the B meson and the pseudoscalar (vector) meson, respectively. The weak vector and axial vector currents are parametrized as [28]

$$\begin{aligned}
\langle D(v') | \bar{c} \gamma_\mu b | B(v) \rangle &= \sqrt{m_B m_D} \left[h_+(\omega) (v + v')_\mu + h_-(\omega) (v - v')_\mu \right], \\
\langle D^*(v', \epsilon') | \bar{c} \gamma_\mu b | B(v) \rangle &= i \sqrt{m_B m_D} h_V(\omega) \varepsilon_{\mu\nu\alpha\beta} \epsilon'^{\nu} v'^\alpha v^\beta, \\
\langle D^*(v', \epsilon') | \bar{c} \gamma_\mu \gamma_5 b | B(v) \rangle &= \sqrt{m_B m_D} \left[h_{A_1}(\omega) (\omega + 1) \epsilon'^*_\mu - h_{A_2}(\omega) \epsilon'^* \cdot v v_\mu \right. \\
&\quad \left. - h_{A_3}(\omega) \epsilon'^* \cdot v v'_\mu \right], \tag{C1}
\end{aligned}$$

where the kinematic variable $\omega = v_B \cdot v_{(D, D^*)} = (m_B^2 + m_{(D, D^*)}^2 - q^2) / 2 m_B m_{(D, D^*)}$. Now, for the $B \rightarrow D$ form factors $F_+(q^2)$ and $F_0(q^2)$, we obtain

$$F_+(q^2) = \frac{V_1(\omega)}{r_D}, \quad F_0(q^2) = \frac{(1 + \omega) r_D}{2} S_1(\omega), \tag{C2}$$

where $V_1(\omega)$ and $S_1(\omega)$, taken from Ref. [29], are

$$\begin{aligned}
V_1(\omega) &= \left[h_+(\omega) - \frac{(1 - r)}{(1 + r)} h_-(\omega) \right], \\
S_1(\omega) &= \left[h_+(\omega) - \frac{(1 + r)(\omega - 1)}{(1 - r)(\omega + 1)} h_-(\omega) \right], \tag{C3}
\end{aligned}$$

and

$$r_D = \frac{2\sqrt{m_B m_D}}{(m_B + m_D)}, \quad r = \frac{m_D}{m_B}. \tag{C4}$$

We follow Ref. [30] and parametrized $V_1(\omega)$ in terms of ρ_1 and z parameters as

$$V_1(\omega) = V_1(1) \left[1 - 8\rho_1^2 z + (51\rho_1^2 - 10)z^2 - (252\rho_1^2 - 84)z^3 \right], \tag{C5}$$

where $z = (\sqrt{\omega + 1} - \sqrt{2}) / (\sqrt{\omega + 1} + \sqrt{2})$. The numerical value of $V_1(1)$ and ρ_1^2 are [38]

$$\begin{aligned}
V_1(1) |V_{cb}| &= (43.0 \pm 1.9 \pm 1.4) \times 10^{-3}, \\
\rho_1^2 &= 1.20 \pm 0.09 \pm 0.04. \tag{C6}
\end{aligned}$$

The form factor $S_1(\omega)$ has the following parametrization [30].

$$S_1(\omega) = 1.0036[1 - 0.0068(\omega - 1) + 0.0017(\omega - 1)^2 - 0.0013(\omega - 1)^3]V_1(\omega). \tag{C7}$$

We now concentrate on the $B \rightarrow V$ i.e. $B \rightarrow D^*$ form factor in the HQET [14] by defining the universal form factor h_{A_1} which can be related to $A_0(q^2)$, $A_1(q^2)$, $A_2(q^2)$, and $V(q^2)$ as

$$A_1(q^2) = r_{D^*} \frac{\omega + 1}{2} h_{A_1}(\omega),$$

$$\begin{aligned}
A_0(q^2) &= \frac{R_0(\omega)}{r_{D^*}} h_{A_1}(\omega), \\
A_2(q^2) &= \frac{R_2(\omega)}{r_{D^*}} h_{A_1}(\omega), \\
V_0(q^2) &= \frac{R_1(\omega)}{r_{D^*}} h_{A_1}(\omega)
\end{aligned} \tag{C8}$$

where $r_{D^*} = 2\sqrt{m_B m_{D^*}}/(m_B + m_{D^*})$. The ω dependence of the form factors in the limit of heavy quark can be written as [14, 29]

$$\begin{aligned}
h_{A_1}(\omega) &= h_{A_1}(1)[1 - 8\rho^2 z + (53\rho^2 - 15)z^2 - (231\rho^2 - 91)z^3], \\
R_1(\omega) &= R_1(1) - 0.12(\omega - 1) + 0.05(\omega - 1)^2, \\
R_2(\omega) &= R_2(1) + 0.11(\omega - 1) - 0.06(\omega - 1)^2, \\
R_0(\omega) &= R_0(1) - 0.11(\omega - 1) + 0.01(\omega - 1)^2,
\end{aligned} \tag{C9}$$

where, we use the following numerical values of the free parameters from Refs. [14, 39] for our numerical analysis. That is

$$\begin{aligned}
h_{A_1}(1) |V_{cb}| &= (34.6 \pm 0.2 \pm 1.0) \times 10^{-3}, \\
\rho_1^2 &= 1.214 \pm 0.034 \pm 0.009, \\
R_1(1) &= 1.401 \pm 0.034 \pm 0.018, \\
R_2(1) &= 0.864 \pm 0.024 \pm 0.008, \\
R_0(1) &= 1.14 \pm 0.114
\end{aligned} \tag{C10}$$

-
- [1] S. Chatrchyan *et al.* [CMS Collaboration], Phys. Lett. B **716**, 30 (2012) [arXiv:1207.7235 [hep-ex]].
 - [2] G. Aad *et al.* [ATLAS Collaboration], Phys. Lett. B **716**, 1 (2012) [arXiv:1207.7214 [hep-ex]]. G. Aad *et al.* [ATLAS Collaboration], Phys. Rev. D **86**, 032003 (2012) [arXiv:1207.0319 [hep-ex]].
 - [3] I. Adachi *et al.* [Belle Collaboration], Phys. Rev. Lett. **110**, 131801 (2013) [arXiv:1208.4678 [hep-ex]].
 - [4] J. P. Lees *et al.* [BaBar Collaboration], arXiv:1207.0698 [hep-ex].
 - [5] J. Beringer *et al.* (Particle Data Group), Phys. Rev. D **86**, 010001 (2012)
 - [6] J. Charles, O. Deschamps, S. Descotes-Genon, R. Itoh, H. Lacker, A. Menzel, S. Monteil and V. Niess *et al.*, Phys. Rev. D **84**, 033005 (2011) [arXiv:1106.4041 [hep-ph]]

- [7] J. Charles *et al.* [CKMfitter Group Collaboration], Eur. Phys. J. C **41**, 1 (2005) [hep-ph/0406184].
- [8] M. Bona *et al.* [UTfit Collaboration], Phys. Lett. B **687**, 61 (2010) [arXiv:0908.3470 [hep-ph]].
- [9] P. del Amo Sanchez *et al.* [BaBar Collaboration], Phys. Rev. D **83**, 032007 (2011) [arXiv:1005.3288 [hep-ex]].
- [10] H. Ha *et al.* [BELLE Collaboration], Phys. Rev. D **83**, 071101 (2011) [arXiv:1012.0090 [hep-ex]].
- [11] D. Asner *et al.* [Heavy Flavor Averaging Group Collaboration], arXiv:1010.1589 [hep-ex].
- [12] S. Fajfer, J. F. Kamenik, I. Nisandzic and J. Zupan, Phys. Rev. Lett. **109**, 161801 (2012) [arXiv:1206.1872 [hep-ph]].
- [13] J. P. Lees *et al.* [BaBar Collaboration], Phys. Rev. Lett. **109**, 101802 (2012) [arXiv:1205.5442 [hep-ex]].
- [14] S. Fajfer, J. F. Kamenik and I. Nisandzic, Phys. Rev. D **85**, 094025 (2012) [arXiv:1203.2654 [hep-ph]].
- [15] G. C. Branco, P. M. Ferreira, L. Lavoura, M. N. Rebelo, M. Sher and J. P. Silva, Phys. Rept. **516**, 1 (2012) [arXiv:1106.0034 [hep-ph]].
- [16] W. S. Hou, Phys. Rev. D **48**, 2342 (1993). A. G. Akeroyd and S. Recksiegel, J. Phys. G **29**, 2311 (2003) [hep-ph/0306037]. M. Tanaka, Z. Phys. C **67**, 321 (1995) [hep-ph/9411405]. U. Nierste, S. Trine and S. Westhoff, Phys. Rev. D **78**, 015006 (2008) [arXiv:0801.4938 [hep-ph]].
- [17] T. Miki, T. Miura and M. Tanaka, hep-ph/0210051.; A. Wahab El Kaffas, P. Osland and O. M. Ogreid, Phys. Rev. D **76**, 095001 (2007) [arXiv:0706.2997 [hep-ph]].; O. Deschamps, S. Descotes-Genon, S. Monteil, V. Niess, S. T’Jampens and V. Tisserand, Phys. Rev. D **82**, 073012 (2010) [arXiv:0907.5135 [hep-ph]].; G. Blankenburg and G. Isidori, Eur. Phys. J. Plus **127**, 85 (2012) [arXiv:1107.1216 [hep-ph]].; G. D’Ambrosio, G. F. Giudice, G. Isidori and A. Strumia, Nucl. Phys. B **645**, 155 (2002) [hep-ph/0207036].; A. J. Buras, M. V. Carlucci, S. Gori and G. Isidori, JHEP **1010**, 009 (2010) [arXiv:1005.5310 [hep-ph]].; A. Pich and P. Tuzon, Phys. Rev. D **80**, 091702 (2009) [arXiv:0908.1554 [hep-ph]].; M. Jung, A. Pich and P. Tuzon, JHEP **1011**, 003 (2010) [arXiv:1006.0470 [hep-ph]].
- [18] A. Crivellin, C. Greub and A. Kokulu, Phys. Rev. D **86**, 054014 (2012) [arXiv:1206.2634 [hep-ph]].
- [19] A. Datta, M. Duraissamy and D. Ghosh, Phys. Rev. D **86**, 034027 (2012) [arXiv:1206.3760 [hep-ph]].
- [20] M. Duraissamy and A. Datta, arXiv:1302.7031 [hep-ph].
- [21] P. Biancofiore, P. Colangelo and F. De Fazio, Phys. Rev. D **87**, 074010 (2013) [arXiv:1302.1042 [hep-ph]].
- [22] A. Crivellin, Phys. Rev. D **81**, 031301 (2010) [arXiv:0907.2461 [hep-ph]].
- [23] A. Celis, M. Jung, X. -Q. Li and A. Pich, JHEP **1301**, 054 (2013) [arXiv:1210.8443 [hep-ph]].

- [24] X. -G. He and G. Valencia, Phys. Rev. D **87**, 014014 (2013) [arXiv:1211.0348 [hep-ph]].
- [25] T. Bhattacharya, V. Cirigliano, S. D. Cohen, A. Filipuzzi, M. Gonzalez-Alonso, M. L. Graesser, R. Gupta and H. -W. Lin, Phys. Rev. D **85**, 054512 (2012) [arXiv:1110.6448 [hep-ph]].
- [26] V. Cirigliano, J. Jenkins and M. Gonzalez-Alonso, Nucl. Phys. B **830**, 95 (2010) [arXiv:0908.1754 [hep-ph]].
- [27] A. Khodjamirian, T. Mannel, N. Offen and Y. -M. Wang, Phys. Rev. D **83**, 094031 (2011) [arXiv:1103.2655 [hep-ph]].
- [28] A. F. Falk and M. Neubert, Phys. Rev. D **47**, 2965 (1993) [hep-ph/9209268].; A. F. Falk and M. Neubert, Phys. Rev. D **47**, 2982 (1993) [hep-ph/9209269].
- [29] I. Caprini, L. Lellouch and M. Neubert, Nucl. Phys. B **530**, 153 (1998) [hep-ph/9712417].
- [30] Y. Sakaki and H. Tanaka, Phys. Rev. D **87**, 054002 (2013) [arXiv:1205.4908 [hep-ph]].
- [31] J. G. Korner and G. A. Schuler, Z. Phys. C **46**, 93 (1990).
- [32] A. Kadeer, J. G. Korner and U. Moosbrugger, Eur. Phys. J. C **59**, 27 (2009) [hep-ph/0511019].
- [33] G. Buchalla, A. J. Buras and M. E. Lautenbacher, Rev. Mod. Phys. **68**, 1125 (1996) [hep-ph/9512380].
- [34] A. Bazavov *et al.* [Fermilab Lattice and MILC Collaborations], Phys. Rev. D **85**, 114506 (2012) [arXiv:1112.3051 [hep-lat]].
- [35] H. Na, C. J. Monahan, C. T. H. Davies, R. Horgan, G. P. Lepage and J. Shigemitsu, Phys. Rev. D **86**, 034506 (2012) [arXiv:1202.4914 [hep-lat]].
- [36] <http://www.latticeaverages.org/>
- [37] D. Choudhury, D. K. Ghosh and A. Kundu, Phys. Rev. D **86**, 114037 (2012) [arXiv:1210.5076 [hep-ph]].
- [38] B. Aubert *et al.* [BaBar Collaboration], Phys. Rev. Lett. **104**, 011802 (2010) [arXiv:0904.4063 [hep-ex]].
- [39] W. Dungen *et al.* [Belle Collaboration], Phys. Rev. D **82**, 112007 (2010) [arXiv:1010.5620 [hep-ex]].
- [40] A. Khodjamirian, R. Ruckl, S. Weinzierl and O. I. Yakovlev, Phys. Lett. B **410**, 275 (1997) [hep-ph/9706303].; E. Bagan, P. Ball and V. M. Braun, Phys. Lett. B **417**, 154 (1998) [hep-ph/9709243].; P. Ball, JHEP **9809**, 005 (1998) [hep-ph/9802394].; P. Ball and R. Zwicky, Phys. Rev. D **71**, 014015 (2005) [hep-ph/0406232].; G. Duplancic, A. Khodjamirian, T. Mannel, B. Melic and N. Offen, JHEP **0804**, 014 (2008) [arXiv:0801.1796 [hep-ph]].
- [41] E. Dalgic, A. Gray, M. Wingate, C. T. H. Davies, G. P. Lepage and J. Shigemitsu, Phys. Rev. D

73, 074502 (2006) [Erratum-ibid. D **75**, 119906 (2007)] [hep-lat/0601021].; J. A. Bailey, C. Bernard, C. E. DeTar, M. Di Pierro, A. X. El-Khadra, R. T. Evans, E. D. Freeland and E. Gamiz *et al.*, Phys. Rev. D **79**, 054507 (2009) [arXiv:0811.3640 [hep-lat]]. A. Al-Haydari *et al.* [QCDSF Collaboration], Eur. Phys. J. A **43**, 107 (2010) [arXiv:0903.1664 [hep-lat]].